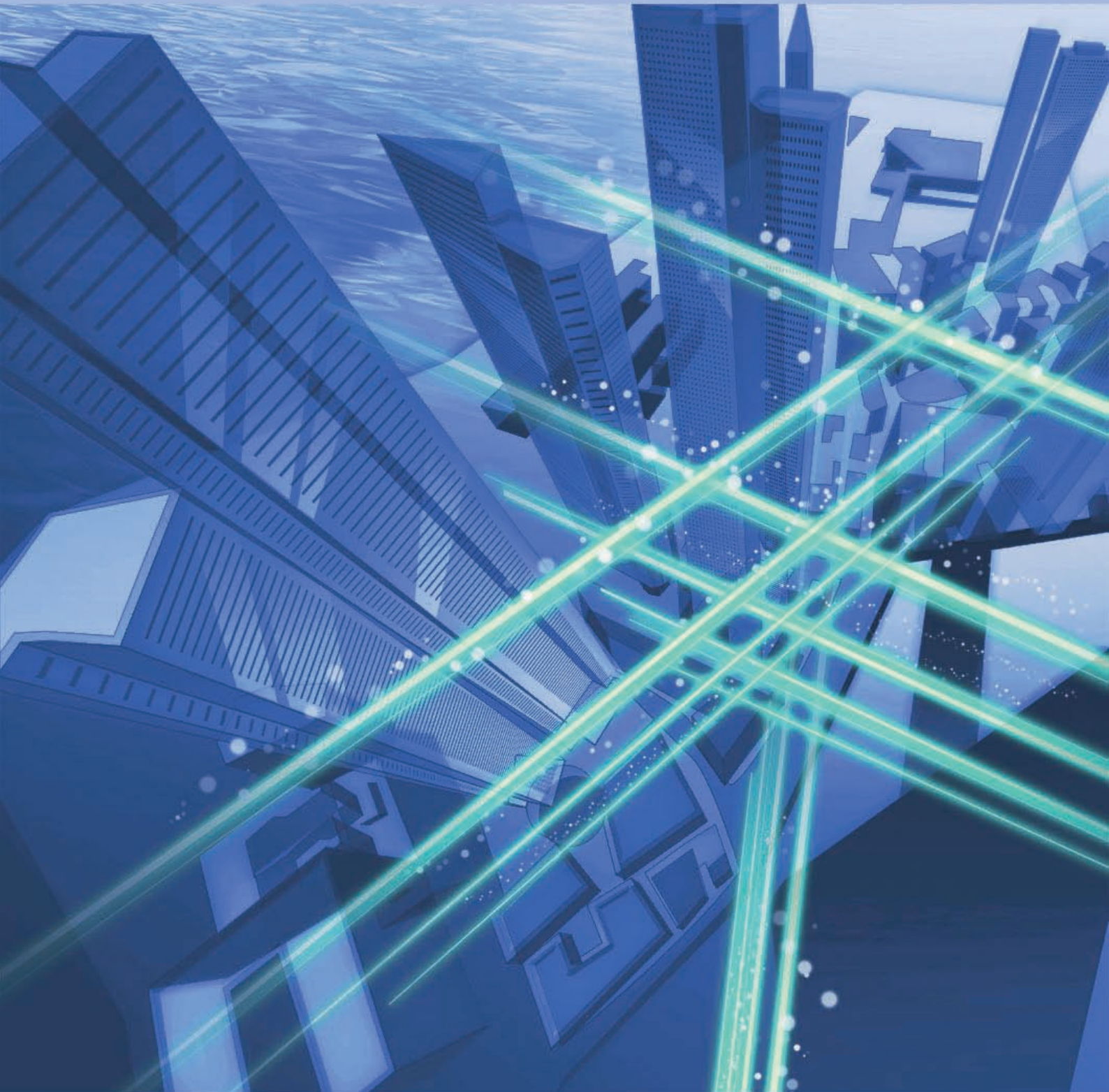


NTT Technical Review

6

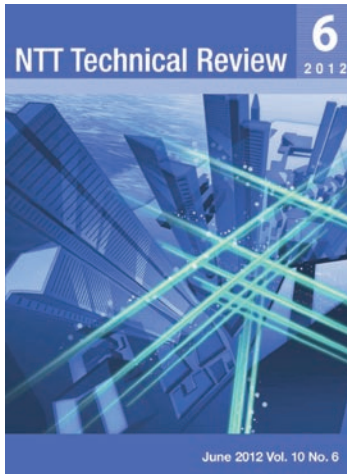
2012



June 2012 Vol. 10 No. 6

NTT Technical Review

June 2012 Vol. 10 No. 6



Feature Article: Latest Development Trend at NTT Access Network Service Systems Laboratories

Technology for Reconnecting Optical Fiber Cable in Existing Aerial Closures

Versatile Optical Fiber Cabling Technologies for Existing Buildings

Direct Spectrum Division Transmission for High-capacity Satellite Communications

Regular Articles

4.6- μ m-band Light Source for Greenhouse Gas Detection

Jubatus: Scalable Distributed Processing Framework for Realtime Analysis of Big Data

Global Standardization Activities

Standardization Activities Related to Machine-to-Machine Communications

Practical Field Information about Telecommunication Technologies

Cable Damage during Deicing of a Handhole

External Awards

External Awards

Technology for Reconnecting Optical Fiber Cable in Existing Aerial Closures

Chihiro Suzuki[†], Yuji Takahashi, Atsushi Hamaoka, and Kazutoshi Takamizawa

Abstract

We have developed a technology for connecting short remnant lengths of optical fiber that enables the reconnection of optical fiber cable in existing aerial drop closures, which is currently difficult because the remnant length is insufficient.

1. Introduction

The number of broadband contracts in Japan reached 36 million in September 2011. Among those, the number of fiber-to-the-home (FTTH) contracts exceeded 21 million, which is more than half the total number of all broadband service contracts (59%) [1]. Accompanying these trends, there have been changes to other services because of service diversification and because of service transfer or termination when customers move home and so forth. For the convenience of new residents and for efficient connection work when services are transferred or cancelled, some of the cabling facilities are left in place, but this has the drawback of lowering the utilization rate of existing facilities. To counter this problem and make more efficient use of existing facilities, we have developed an optical fiber cable reconnection technology that enables the reconnection of optical fibers remaining in aerial drop closures [2] after an optical fiber drop connection has been cut.

2. Concept

To enable optical services to be offered to customers at their residences, aerial distribution closures are commonly used. Each one is fitted off-site in advance with an optical splitter of appropriate capacity. When service is newly provided to a customer, an optical

fiber cable (drop cable) is fed to the customer's residence from an aerial optical drop closure, which is connected to the aerial distribution closure via a distribution cable (**Fig. 1**).

The aerial drop closure at a customer's residence is often an AOF or AOF24 closure (**Fig. 2**). These closures are compact and economical facilities that can be installed as demand arises. However, in order to improve their drop cabling workability, optical core fibers pass through the aerial drop closure in straight lengths. When a drop cable is installed and connected to the upstream-side (central-office side) cable via an FAS (field assembly small-sized) connector, the optical fiber cable in the closure is cut, an FAS connector socket is attached to the upstream-side fiber and connected to the FAS connector plug of the drop cable, and a short remnant length of the downstream-side optical fiber is left inside the closure. However, once the optical fiber has been cut, reconnection of the upstream and downstream optical fibers has, until now, been difficult owing to the short length of downstream-side optical fiber remaining in the closure. This is because, when an FAS connector is installed, some of the upstream-side cable is lost since the fiber must be trimmed with a fiber cutter. With the straight-fiber configuration, reconnection of the upstream- and downstream-side fibers is impossible using this shortened length of core fiber, as shown in Fig. 2(c): even after a connector has been attached, the optical fiber does not reach the connector (in the case of existing connectors). Reconnection is enabled (Fig. 2(d)) by a newly developed patch fiber, as explained

[†] NTT Access Network Service Systems Laboratories
Tsukuba-shi, 305-0805 Japan

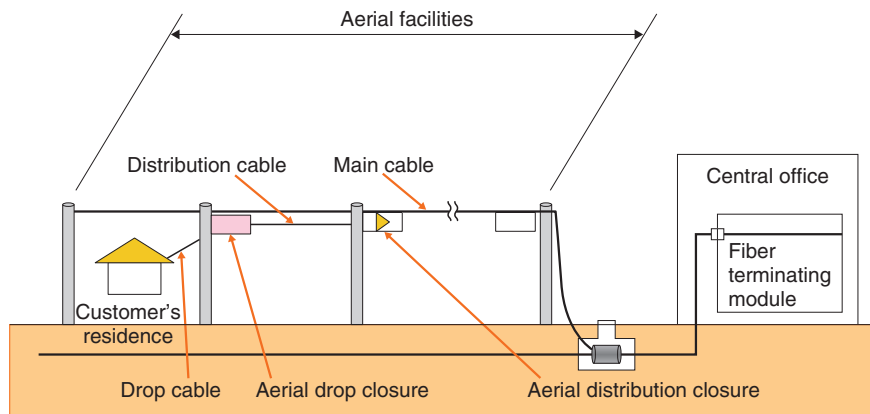


Fig. 1. Configuration of Japanese FTTH service facilities.

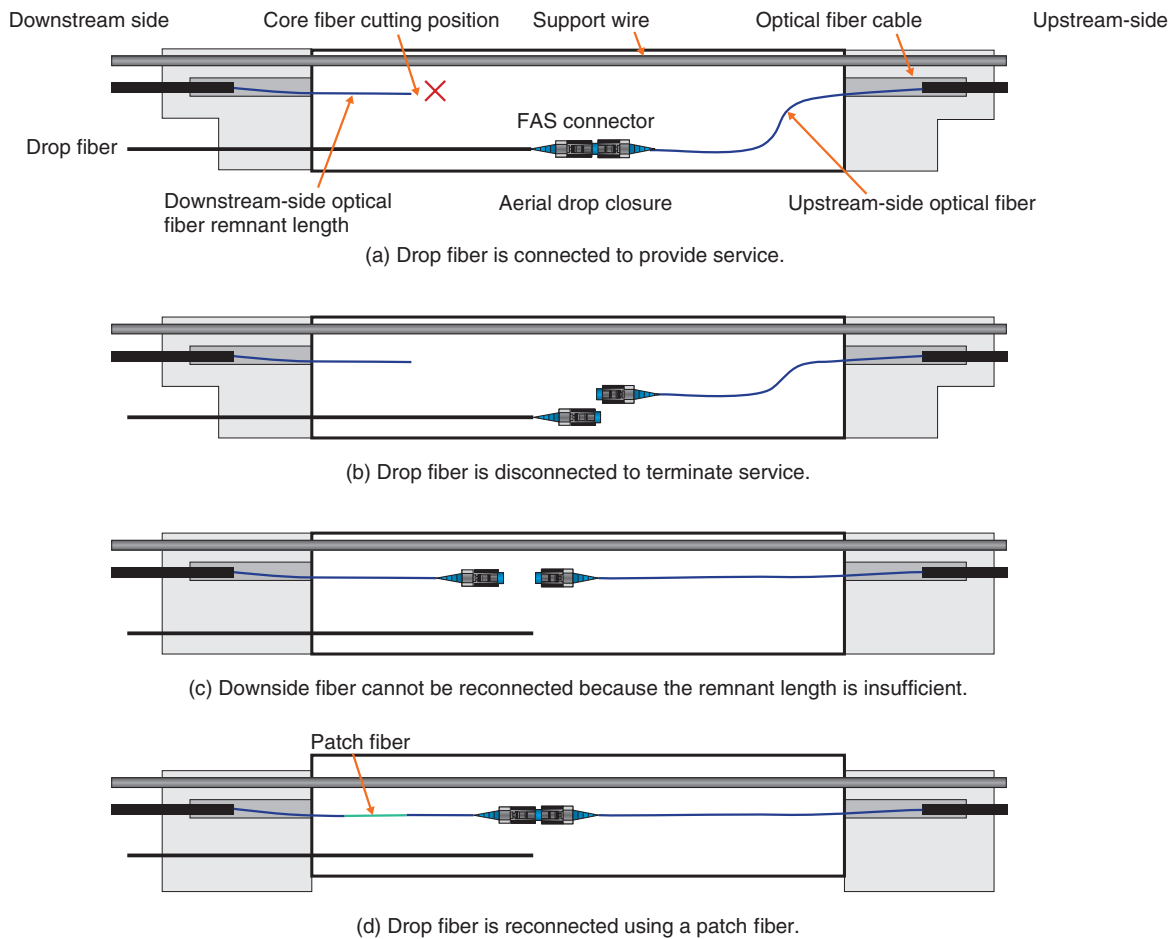


Fig. 2. Structure of closure (in the case of both AOF and AOF24).

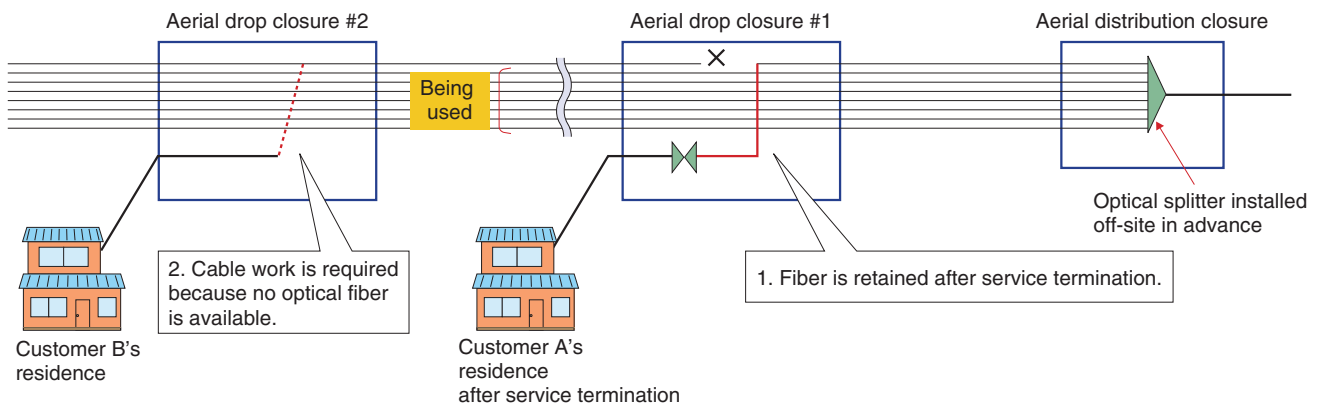


Fig. 3. Problem.

in section 3.1.

The problem is illustrated in **Fig. 3**. When service was supplied to Customer A, one of the eight fibers from the splitter in the aerial distribution closure was cut in drop closure #1 and a drop cable was installed. Later, customer A terminated the service contract, but the cut downstream fiber is not available to other customers. For example, consider the situation when Customer B further downstream requests service. Although seven of the fibers in drop closure #2 are in use, one fiber is not being used; however, it is not connected to the NTT central office because it was cut further upstream in drop closure #1. Until now, the only way to provide service to Customer B has been to lay additional cable, but new optical cabling work is expensive. It would be more efficient and economical if we could utilize the spare fiber in drop closure #2 by reconnecting the cut in drop closure #1. Considering this situation, we identified three needs: (1) a patch fiber that can easily be connected with the remnant lengths of downstream-side optical fibers in aerial drop closures, (2) connectors that can be attached in the empty space in an existing closure without compromising the closure's functions, and (3) fiber protection during the additional stripping of existing cables because workability is especially poor with the shorter remnant lengths of downstream-side optical fibers in AOF closures.

To meet these needs, we have developed an optical aerial closure patch fiber suitable for the 150-mm remnant length in an AOF24 closure and an extension sleeve to adapt it to work with the shorter 80-mm remnant length in an AOF closure. We also developed tools for connecting short remnant lengths and a tray for downstream-side cable reconnection. The patch

fiber enables reconnection of the upstream and downstream fibers, the tray provides mechanical support during this reconnection procedure.

3. Development

3.1 FAS-A patch fiber

We developed two types of patch fibers (called A and B) in order to reconnect an optical fiber (**Fig. 4**). The FAS-A (FAS type A) patch fiber (diameter: 0.5 mm) has an FAS connector plug at one end and a mechanical splice at the other end. The FAS connector plug is designed to mate with the FAS connector socket added to the upstream-side optical fiber in the closure when the optical fiber drop cable was installed. The mechanical splice is a two-sided joint which is connected to the patch fiber on one side and open the other side. The FAS-A patch cable is factory-assembled for maximum quality. To connect the FAS-A patch fiber to the downstream-side optical fiber, the field technician connects the mechanical splice to the downstream fiber. This requires only a short length of downstream fiber, which makes on-site work more efficient and reduces the number of connection failures and subsequent optical fiber shortening. Furthermore, by designing a short patch fiber, we can avoid the need to store rolled-up fiber and can instead store it straight; this minimizes the space required for storage and ensures good workability.

3.2 Connection tools

To make a connection in the confined space in AOF and AOF24 closures, we have developed short remnant fiber length connection tools that can connect

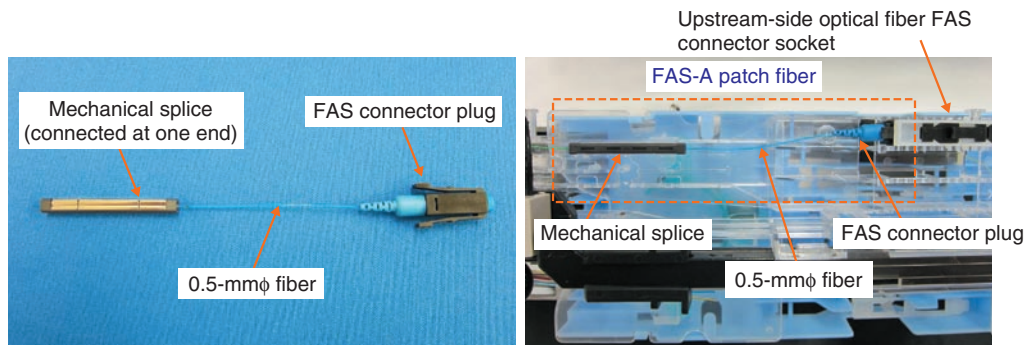
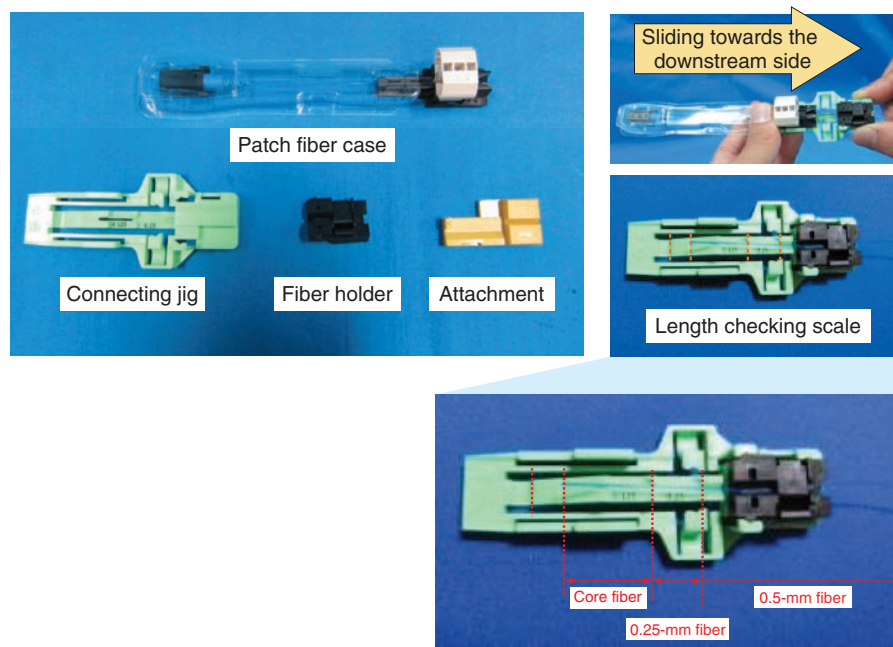


Fig. 4. FAS-A patch fiber.



Remnant length connection tools.

Fig. 5. Short remnant length connection tools.

the short lengths available by moving the patch fiber with the attached mechanical splice toward the fixed remnant length of the downstream-side optical fiber (Fig. 5). The patch fiber is stored in a patch fiber case, and the V-shaped mechanical splice connection is set up in advance. The connection is made simply by pulling the patch fiber out of the case and into the connecting jig, onto which are mounted a fiber holder and an attachment. The improved workability means that a field technician can insert the optical fiber into

the mechanical splice with one hand.

To ensure good workability with the short remnant lengths of optical fiber, we have made the fiber holder as small as possible. We designed the connection procedure in a failsafe manner to ensure that the technician does not perform the procedure incorrectly. We slanted the bottom of the fiber holder so that the technician will feel uncomfortable if he or she does not use the attachment when stripping the sheath or when cutting the fiber. The jig has a length checking scale

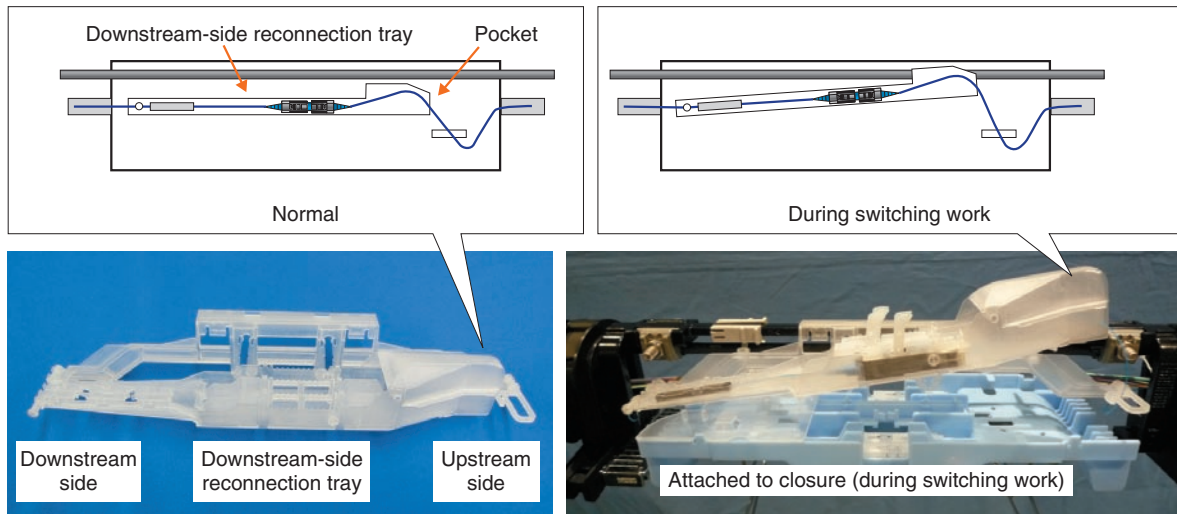


Fig. 6. Downstream-side reconnection tray.

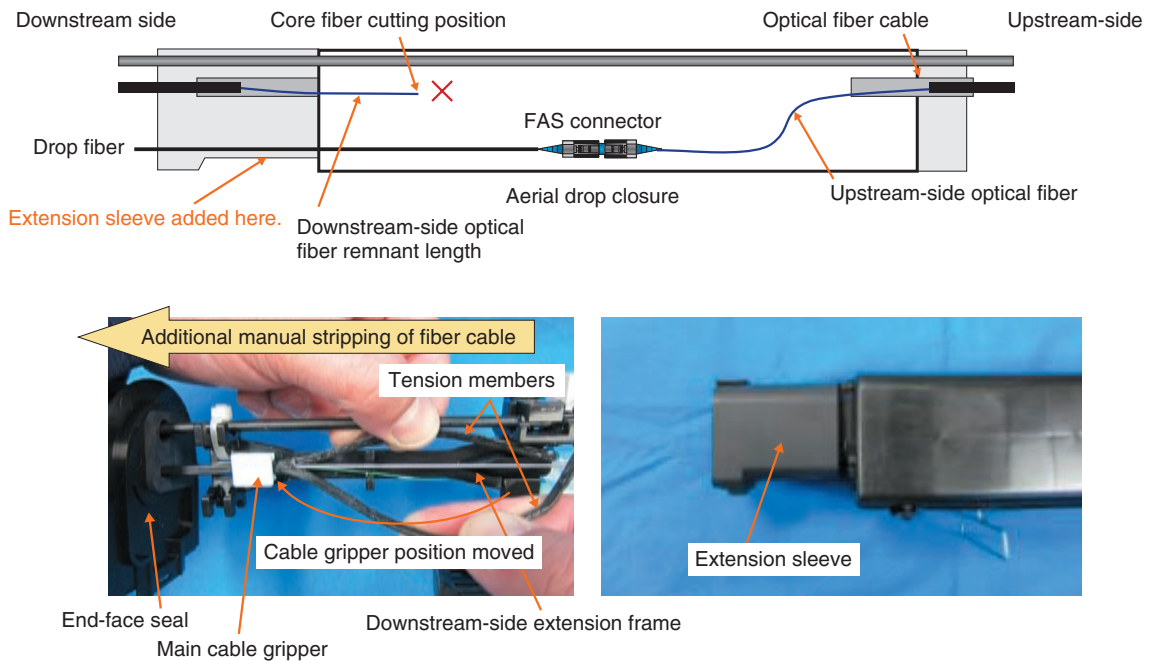


Fig. 7. Extension sleeve.

marked on it so that the technician can ensure that the fiber is the appropriate length without requiring a ruler.

3.3 Downstream-side reconnection tray

The downstream-side reconnection tray is designed to hold the patch fiber and to fit into the empty space

inside the AOF or AOF24 closure (**Fig. 6**). We have ensured workability by storing the optical fiber straight (rather than in a loop), holding the patch fiber connection, and including a pocket to store the extra length of the upstream-side optical fiber. Moreover, the tray structure allows for free positioning and attachment of the upstream FAS connector and

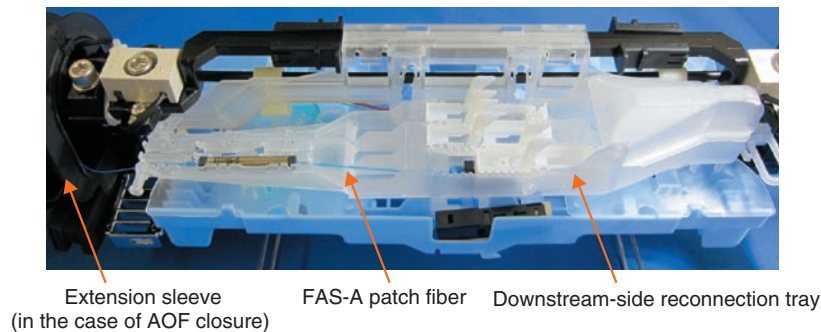


Fig. 8. Technology for reconnecting optical fiber cable in existing aerial closures.

downstream mechanical splice connection. As well as those innovations, we have designed the tray to move up or down by means of a pivot at the mechanical-splice side so that it does not impede reconnection work in the AOF or AOF24 closure or work during the switching of the upstream-side optical fibers.

3.4 Extension sleeve and extension frame for downstream-side extension

With the AOF closure, the remnant length of downstream-side optical fiber is shorter than in the AOF24 closure (80 mm versus 150 mm). In this case, an additional length of the downstream-side optical fiber cable must be pulled into the closure and stripped back until the exposed fiber length is 150 mm, the same as in the case of the AOF24 closure (Fig. 7). The procedure is as follows:

- (1) Slide the AOF closure end-face seal attached to the drop fiber cable downwards.
- (2) Remove the gripper from the existing main cable, attach the downstream-side extension frame to the closure frame, and then secure the cable with the cable gripper.
- (3) Pull the tension members apart by hand to strip the sheath from the cable (no tools required).
- (4) Cut the optical fiber cable sheath and partition.
- (5) Using binders (not shown in Fig. 7), secure the optical fiber cable sheath in order to fix its position.

- (6) To ensure drip-proofing along the section of additional stripping, attach the extension sleeve when the AOF closure end-face seal is moved. We have made the system more economical by making the AOF closure end-face seal reusable.

4. Conclusion

By enabling the reconnection of optical fiber cables in existing AOF and AOF24 closures (Fig. 8), these developments promise efficient use of existing aerial optical cables and will contribute to facility construction and lower operating costs. These short remnant-length optical fiber connection technologies also hold future promise for use in a wide range of other tight-space applications.

References

- [1] Public announcement about the number of broadband contracts and share in Japan (2Q 2011) by Ministry of Internal Affairs and Communications (in Japanese). http://www.soumu.go.jp/main_sosiki/kenkyu/saigai/01kiban04_02000030.html
- [2] M. Kama, M. Toyonaga, N. Ogawa, H. Tanase, M. Awamori, and K. Anzai, "Development of New Aerial Optical Cable and Closure that Allow Subsequent Closure Installation," NTT Technical Review, Vol. 5, No. 8, 2007. <https://www.ntt-review.jp/archive/ntttechnical.php?contents=ntr200708le2.html>



Chihiro Suzuki

Member, Second Promotion Project, NTT Access Network Service Systems Laboratories.

He received the B.E. degree in civil engineering from Nihon University, Tokyo, in 1997. He joined NTT EAST in 1997 and moved to NTT Access Network Service Systems Laboratories in April 2010. Since then, he has been engaged in the development of optical closure technology.



Atsushi Hamaoka

Senior Research Engineer, Second Promotion Project, NTT Access Network Service Systems Laboratories.

He received the B.E. degree in mechanical engineering from Kanagawa University in 1992. He joined NTT in 1992 and moved to NTT Access Network Service Systems Laboratories in August 2008. Since then, he has been engaged in the development of optical closure technology.



Yuji Takahashi

Member, Second Promotion Project, NTT Access Network Service Systems Laboratories.

He received the B.E. degree in electronics and electrical engineering from Hosei University, Tokyo, in 1999. He joined NTT EAST in 1999 and moved to NTT Access Network Service Systems Laboratories in July 2008. Since then, he has been engaged in the development of optical closure technology.



Kazutoshi Takamizawa

Senior Research Engineer, Supervisor, Second Promotion Project, NTT Access Network Service Systems Laboratories.

He received the M.E. degree in electronic engineering from Shinshu University, Nagano, in 1987. He joined NTT in 1987 and is currently engaged in the development of the optical access network.

Versatile Optical Fiber Cabling Technologies for Existing Buildings

Hayato Minami[†], Kazuki Nakano, Keita Kuramoto, Atsushi Daido, Kazutoshi Takamizawa, Tadashi Sasaki, and Tetsuhiro Numata

Abstract

We have developed a *single 8-core low-friction indoor optical cable* for high-precision cabling and a range of enhanced modules (*E modules*), which can be installed as demand requires. These versatile technologies overcome the problems encountered in the provision of optical fiber cabling to customers in small to medium-sized multi-dwelling units owing to the limited free space in existing conduits in customers' buildings. These technologies are also applicable for cabling in large buildings.

1. Introduction

In September 2011, the number of fiber-to-the-home contracts in Japan surpassed 21 million [1]. However, since approximately 42% of Japanese families live in multi-dwelling units (MDUs) [2], optical cabling systems for MDUs have become important. In contrast to FTTH cabling schemes for detached houses, which consist of a 4-branch optical splitter in the central office and 8-branch splitter module parts (SPs) installed on the user side (supporting 32 subscribers), schemes for MDUs and office buildings use 32-branch SPs (or a cascade of one 4-branch SP followed by four 8-branch SPs) [3].

As shown in **Fig. 1**, *small-diameter low-friction indoor optical cables* (hereinafter, narrow indoor cables) that enable multiple cable laying in conduits and *splitter module types suitable for dividable cabinets* (D cabinets) that can be installed in the empty spaces within facilities in MDUs and other buildings (telephone conduits, main distribution frame (MDF) boxes, and so on) have been developed [2]–[4] and implemented to expand the range of available cabling systems. These developments have contributed to a reduction in the number of small and medium-sized

MDU buildings for which no optical fiber cabling systems exist; however, it is still not possible to provide optical services to all customers: as shown in **Fig. 1**, one reason is that customer telephone conduits (especially vertical conduits between floors) are not big enough to accommodate all of the cables required. Therefore, to provide services to even more customers, we need to provide products that enable a flexible response to demand in existing buildings.

2. Development concept

To overcome the cabling difficulties in small to medium-sized MDUs, conventional cabling techniques need to be substantially revised. Some specific cabling systems are shown in **Fig. 2**. Normally, narrow indoor cables are laid in a vertical conduit as customer demand arises, although this depends on the space available in the conduit: it is usually possible to lay one or two cables in a conduit, but it is often difficult to lay more once a conduit has three or more cables. There have also been problems with ensuring space to install distribution modules (module Ds) when laying 4-core indoor optical cables. To tackle these issues, we have developed a *single 8-core low-friction indoor optical cable* (8ST indoor cable). It can be inserted into a vertical conduit in advance and then branched on-demand using optical cables at the

[†] NTT Access Network Service Systems Laboratories
Tsukuba-shi, 305-0805 Japan

MDU size		Small (up to 10 dwellings)	Medium (10–50 dwellings)	Large (50 dwellings or more)	
States of facilities	Space in conduits	Yes	Small-diameter low-friction indoor optical cables		
		No	Conduit in place (but cable cannot be fed in)	Conduit in place (but cable cannot be fed in)	Conduit available/ no conduit (cabling for confined spaces)
Space in MDF boxes	Large ▼ Small None	Multicore indoor optical cables			
		D cabinet			
		Compact cabinets			
		Compact splitters B and C	Cabinet installation in confined spaces		
		Surface-mountable splitters			

: Areas covered more thoroughly by these developments
 : Remaining issues (after these developments)

Fig. 1. Areas covered by the new developments and remaining issues.

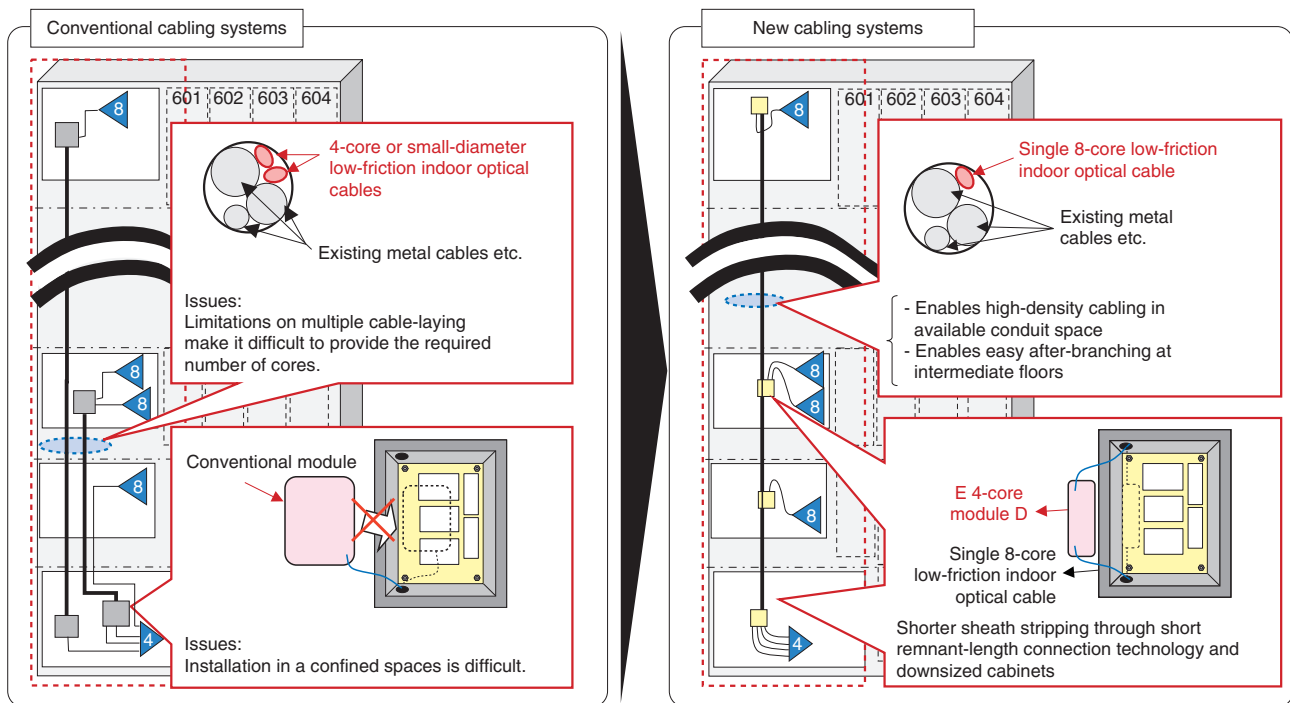


Fig. 2. Comparison of conventional and new cabling systems.

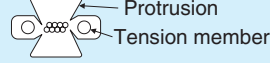
customer’s floor and *space-saving enhanced modules* (E modules) to protect the connection point and the branched optical cables.

2.1 Single 8-core low-friction indoor optical cable

We aimed to create an 8-core indoor optical cable

that can be laid in the space previously taken up by two narrow indoor cables in a narrow conduit and that can be worked with ordinary tools such as nippers for after-branching work. We chose eight cores because this enables service provision to all customers from an 8-branch splitter.

Table 1. Comparison of conventional and new cables.

	Conventional cable (8S-core indoor cable)	New cable (8ST indoor cable)
Shape		
Size	1	1
Friction comparison	1	1/5 Same as small-diameter low-friction indoor cable
Push-feed workability	×	○
After-branching workability	×	○

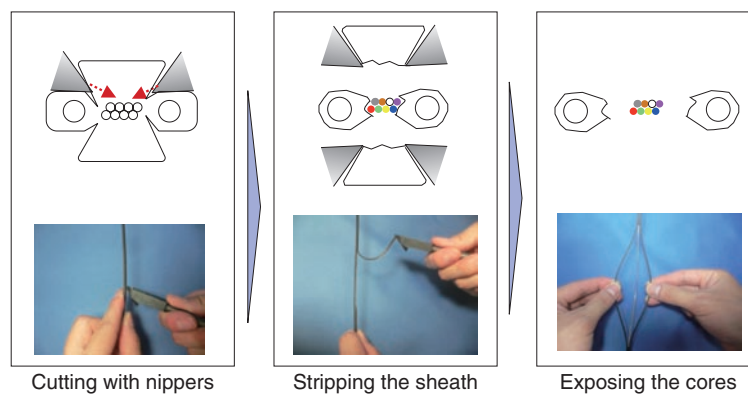


Fig. 3. Stripping the 8ST indoor cable.

The newly developed cable (8ST indoor cable) is compared with the conventional multicore indoor optical cable (8S-core) in **Table 1**. The 8ST cable consists of two tapes, each containing four single-core fibers (S: single-core; T: tape); the 8S cable consists of eight single-core fibers (S: single). The 8ST indoor cable has almost the same external dimensions as the 8S-core indoor cable, but is easier to lay in conduits: we have used a low friction outer sheathing material similar to that used for narrow indoor cables. This lowers the amount of force required to pull or push the cable through a conduit during cable laying work.

In the after-branching of conventional cables, pulling out the desired core from a multicore indoor cable was problematic on intermediate floors with lines in operation. Furthermore, specialized stripping and dividing tools were required to expose the core in aerial cables that can be after-branched. However, as shown in **Fig. 3**, our new cable can be stripped using ordinary tools that service personnel normally have at hand, which avoids the need to equip them with new

specialized tools.

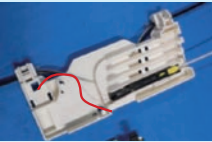
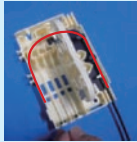
2.2 Enhanced modules (E modules)

With conventional modules, work is needed to pack wires into the module’s housing. To reduce the amount of this work, and in consideration of maintenance, we also aimed to develop modules that can accommodate cable in non-looping lengths.

Our newly developed modules are compared with a conventional one in **Table 2**, where the red lines (guides for the eye) indicate the looped and non-looping storage configurations. As indoor modules for use in conjunction with the 8ST indoor cable, we have developed the enhanced 4-core distribution module (E 4-core module D) that enables up to four cores to be distributed and can be mounted on a post as required and the enhanced 8-core termination module (E 8-core module T) for installation at the cable ends.

To enable cable to be stored inside the module in non-looping lengths (all photographs for new modules except the leftmost (conventional module) in

Table 2. Comparison of conventional and new modules.

	Conventional module	New modules (E modules)		
Installation point	Indoors/outdoors	Indoors		Outdoors
Installation area ratio	1	1/2		1
Installation method	In advance	After installation	In advance	In advance
Cable stripping length	1	1/10 approx.		
Cable packing	Looped cable storage inside the module 	Non-looping cable storage reduces cable packing work		
		 E 4-core module D	 E 8-core module T	 E multicore storage tray (set)

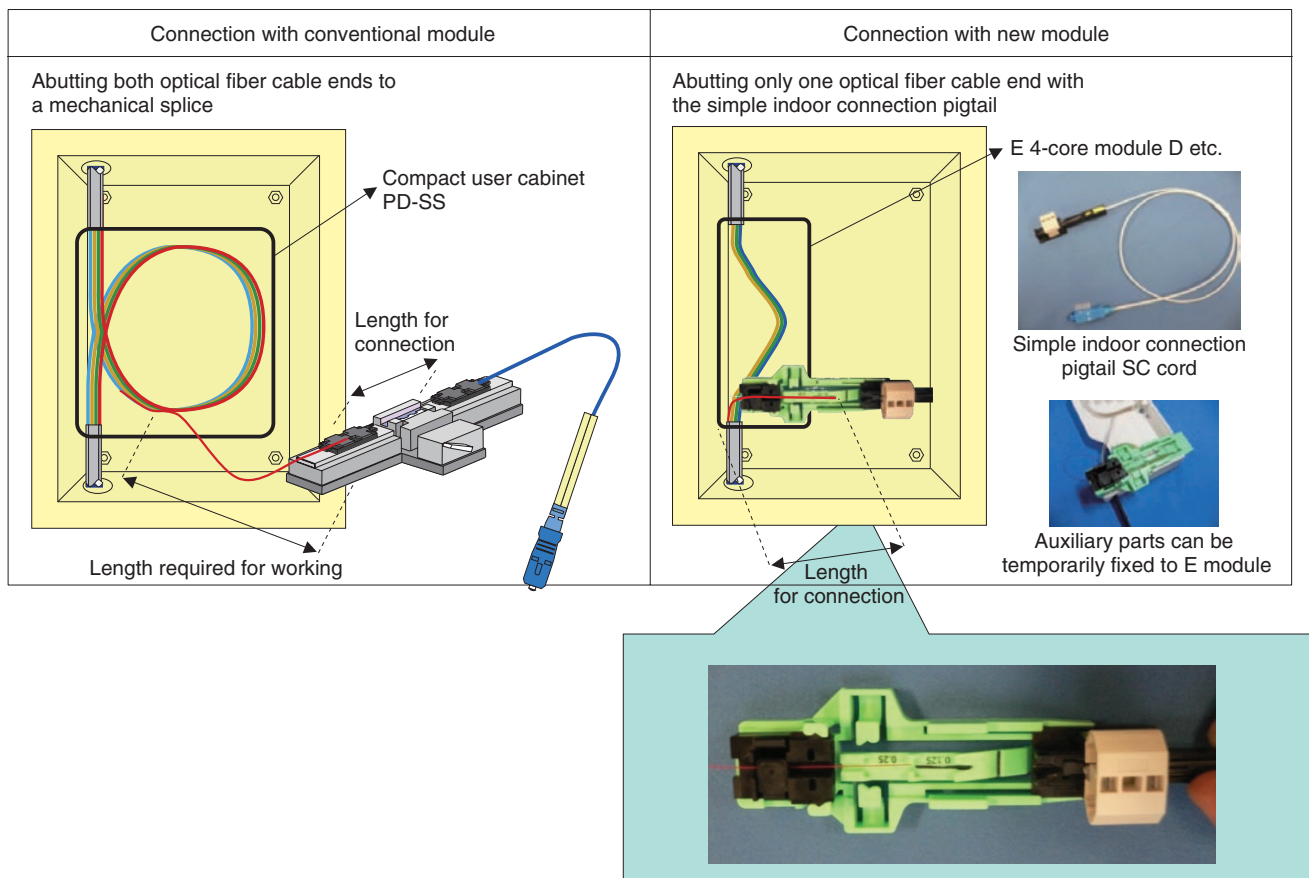


Fig. 4. Comparison of connection methods for conventional and new modules.

Table 2), it was necessary to revise the conventional connection methods. As a result, we developed a simple indoor connection pigtail in which an SC connector cord is attached to a mechanical splice made in

advance, as shown in **Fig. 4**. With conventional modules, approximately 2 m of cable, consisting of the length for connection and the length for working, had to be stripped and packed inside the module. To store

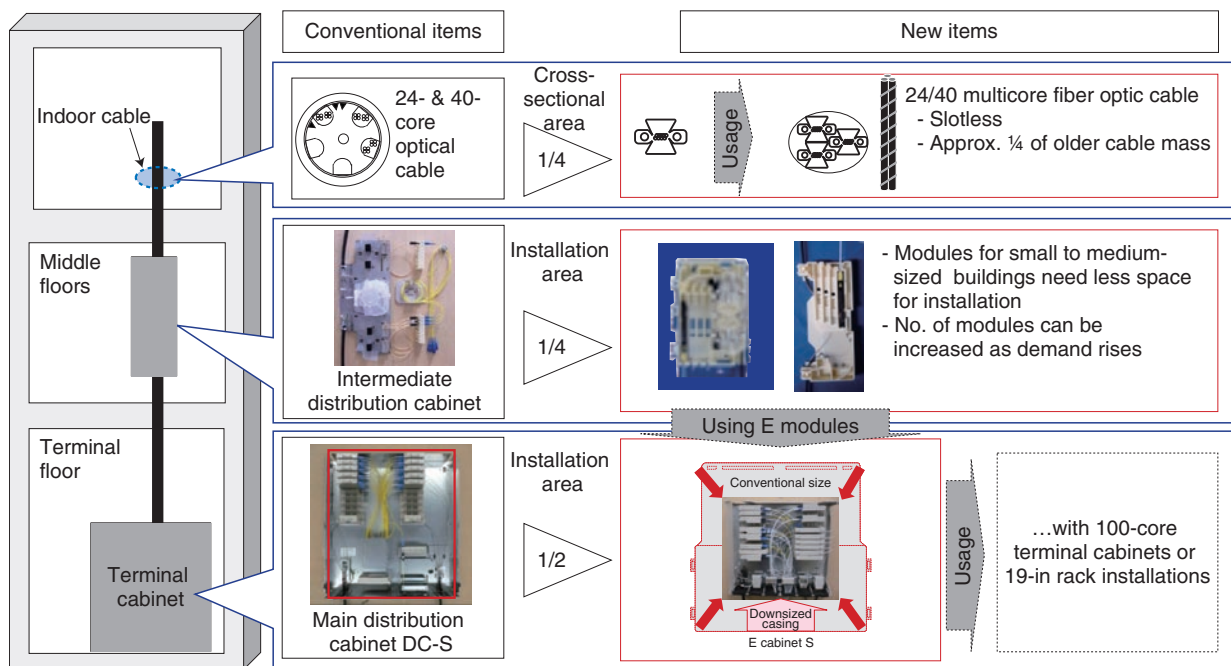


Fig. 5. Comparison of components for application to large buildings.

this fiber without bending it beyond its minimum bending radius, it was packed in a circular loop. With the new modules, on the other hand, the necessary length is only that required for connection; moreover, the length required for connection is shorter, so the length of cable that needs to be stripped is reduced by approximately 90%, enabling non-looping storage. Furthermore, the modules themselves are about 50% smaller than the older versions, so they can be installed in small MDFs and other places.

We have also developed a set of *enhanced multicore storage trays* (E multicore storage trays) for use in conjunction with these modules and cables that can be installed on external walls etc. The E 8-core module T can also be housed in a box that is resistant to ultraviolet light and rain for outdoor installation. Furthermore, wall-mounted splitter modules can be attached to the cover of an E multicore storage tray with screws.

3. Application to large buildings

Currently, slot cable-type cables with 24 or 40 cores and a main distribution cabinet type S (DC-S) are available for buildings that have a large broadband demand such as office blocks. However, the 24- and 40-core optical cables require long lengths to be

stripped, and because of the large size of the DC-S, there have been cases where approval could not be obtained through negotiation with customers. To counter these issues, the new 8ST indoor cable and E modules offer improved workability and better installation potential in large buildings. The new and conventional structures are compared in Fig. 5.

The new 24- and 40-core multifiber cables consist of either three or five 8ST indoor cables bundled together and are approximately 75% lower in mass and smaller in diameter than the older versions. Used in conjunction with the E modules, these cables enable elemental termination or mid-cable connection as required. Moreover, while the older cables can be bent to a radius of 30 mm, the new version can tolerate being bent to a radius of 15 mm, which greatly improves cabling workability.

E cabinets house E modules in cases that are the same size as those used in the conventional cabinets (PT cabinets). In this way, the workability of the D cabinet is retained, while the area required for installation is reduced by 50%. We have made the connection method simpler with the simple indoor connection pigtail. Modules that can be installed in the E cabinet can also be installed on shelving in existing D cabinet racks. Moreover, the cable grippers in PT cabinets can be opened wider than usual, so these

newly developed items are compatible with existing systems. Moreover, with cabinets, we are considering ways to mount the items in trays for 19-inch rack installations designed to meet high demand.

4. Future plans

We will support the speedy deployment and expansion of services by improving workability in existing conduits between floors in MDUs through the introduction of the optical cabling technologies that we have developed. We intend to phase out existing cabinet products through the deployment of the cabinet products introduced in this article.

References

- [1] Quarterly Data on Telecommunications Service Contract Numbers and Market Share—Telecommunication Bureau of the Ministry of Internal Affairs and Communications (in Japanese).
http://www.soumu.go.jp/main_sosiki/kenkyu/saigai/01kiban04_02000030.html
- [2] Statistics Bureau, Ministry of Internal Affairs and Communications: “Housing and Land Survey 2008”.
<http://www.stat.go.jp/english/data/jyutaku/results.htm>
- [3] H. Minami, K. Shiraishi, T. Sasaki, K. Takamizawa, T. Numata, and O. Inoue, “Cabling Technologies Providing More Optical Cabling Potential in Multi-dwelling Unit Buildings,” NTT Technical Review, Vol. 9, No. 6, 2011.
<https://www.ntt-review.jp/archive/ntttechnical.php?contents=ntr201106ra1.html>
- [4] K. Anzai, N. Toyota, T. Yamamoto, D. Kurematsu, S. Tetsutani, N. Ogawa, K. Shiraki, and K. Takamizawa, “Expansion of Applicability of Multiple Cabling Technology,” NTT Technical Review, Vol. 2, No. 2, 2009.
<https://www.ntt-review.jp/archive/ntttechnical.php?contents=ntr200902le1.html>
- [5] S. Niwa, H. Minami, K. Takamizawa, Y. Takeshita, and T. Handa, “Development of New Optical Wiring Technology for Multi-dwelling Unit Buildings,” NTT Technical Review, Vol. 7, No. 9, 2009.
<https://www.ntt-review.jp/archive/ntttechnical.php?contents=ntr200909le1.html>



Hayato Minami

Research Engineer, NTT Access Network Service Systems Laboratories.

He joined NTT in 2006. Since moving to NTT Access Network Service Systems Laboratories in 2008, he has been engaged in the development of systems for optical wiring techniques for MDUs.



Kazutoshi Takamizawa

Senior Research Engineer, Supervisor, Second Promotion Project, NTT Access Network Service Systems Laboratories.

He received the M.E. degree in electronic engineering from Shinshu University, Nagano, in 1987. He joined NTT in 1987 and is currently engaged in the development of the optical access network.



Kazuki Nakano

Research Engineer, NTT Access Network Service Systems Laboratories.

He joined NTT in 2010. Recently, he has been engaged in the development of systems for optical wiring techniques for MDUs.



Tadashi Sasaki

Section Chief, NTT EAST-TOKYO CORPORATION.

He joined NTT in 1985. Recently, he has been engaged in the development of systems for optical wiring techniques for MDUs. At the time of the research reported in this article, he was a research engineer in NTT Access Network Service Systems Laboratories. He moved to NTT EAST-TOKYO CORPORATION in October 2011.



Keita Kuramoto

Research Engineer, NTT Access Network Service Systems Laboratories.

He joined NTT in 2011. Recently, he has been engaged in the development of systems for optical wiring techniques for MDUs and fiber drop cables.



Tetsuhiro Numata

Department Head, NTT EAST-TOKYO CORPORATION.

He joined NTT in 1990. Recently, he has been engaged in the development of systems for optical wiring techniques for MDUs. At the time of the research reported in this article, he was a senior research engineer and supervisor in NTT Access Network Service Systems Laboratories. He moved to NTT EAST-TOKYO CORPORATION in July 2011.



Atsushi Daido

Research Engineer, NTT Access Network Service Systems Laboratories.

He joined NTT in 1994. Recently, he has been engaged in the development of systems for optical wiring techniques for MDUs.

Direct Spectrum Division Transmission for High-capacity Satellite Communications

Jun-ichi Abe[†], Katsuya Nakahira, Yoshinori Suzuki, and Takatoshi Sugiyama

Abstract

We investigated direct spectrum division transmission (DSDT) for satellite communications. A DSDT-based satellite communication system can be made by modifying the design of the existing satellite communication system by inserting a DSDT adapter between the modem and antenna. On the transmitter side, the DSDT adapter divides the modem's output signal into multiple sub-spectra and assigns them to unused frequency resources. On the receiver side, the divided sub-spectra are combined and the original signal is regenerated. Therefore, the DSDT system utilizes existing satellite communication system components and achieves higher frequency utilization efficiency. Experiments on a prototype DSDT adapter show that its resulting bit error rate performance is close to that in the case without spectrum division. The results demonstrate that the DSDT adapter achieves flexible spectrum division and hence enables high-capacity satellite communications.

1. Introduction

Much of eastern Japan was severely impacted by the Great East Japan Earthquake on March 11, 2011. Many cities were destroyed by tsunami, liquefaction, and subsidence. Since terrestrial communication systems were also seriously damaged, satellite communications became essential in afflicted areas. Before the disaster, satellite communications was being used to provide telephone and fax services, but after the disaster, Internet connectivity was the dominant demand [1]. However, since frequency resources are limited, Internet connection services must share the bandwidth with existing telephone and fax services.

In typical satellite communication systems, demand assigned multiple access (DAMA) provides the frequency resources of the satellite transponder to user earth stations (UESs). Since each UES releases its assigned frequency resources after disconnection, the

transponder's unused frequency resources, which may not be wide enough to be reallocated to new users, become scattered. This fragmentation of the frequency resources seriously degrades frequency utilization efficiency. Moreover, existing satellite communication devices need to be used efficiently because of their long life cycle.

This article introduces the concept of direct spectrum division transmission (DSDT) for satellite communications [2], [3]. A DSDT-based satellite communication system can be made by modifying the design of the existing satellite communication system by inserting a DSDT adapter between the modem and antenna. On the transmitter (Tx) side, the DSDT adapter divides the output signal of the existing modem into multiple sub-spectra in the frequency domain and assigns them to unused frequency resources according to the frequency usage load on the satellite transponder. Therefore, the DSDT system has higher frequency utilization efficiency than the existing system. On the receiver (Rx) side, divided sub-spectra are combined and the original signal is

[†] NTT Access Network Service Systems Laboratories
Yokosuka-shi, 239-0847 Japan

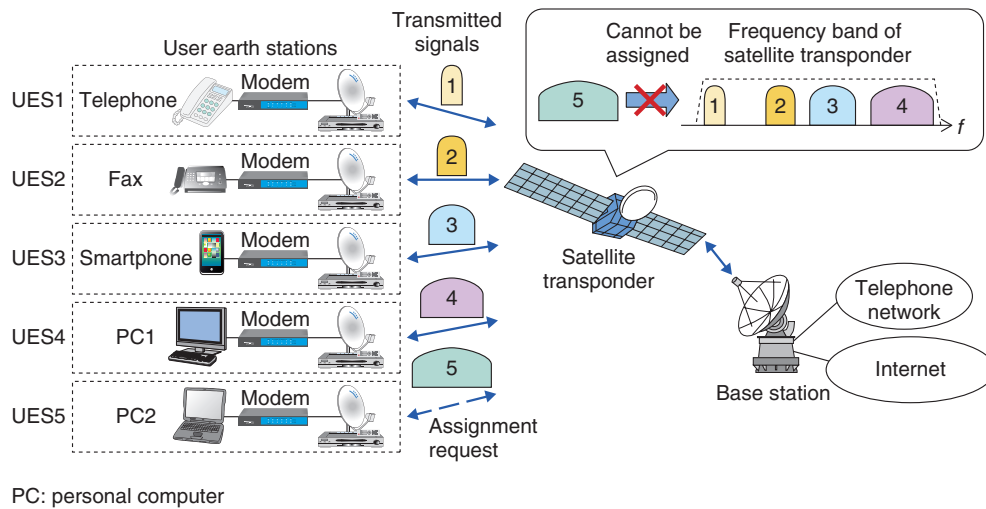


Fig. 1. Overview of current satellite communication system.

regenerated in the DSDT adapter. The regenerated signal is demodulated by the existing Rx modem.

This article explains the concept and principle of DSDT and describes an experimental evaluation of the performance of a prototype DSDT adapter.

2. Key issue

The conventional DAMA-based satellite communication system is shown in Fig. 1. User terminals, such as telephones, faxes, smartphones, and personal computers, are connected to the UESs. Telephone and Internet connections are provided via the satellite transponder and the base station. For the duration of its communication session, each user is assigned a transmission channel with a different frequency, and the modem of the UES outputs a signal with a single carrier frequency modulated by the data to be transmitted. Consider the case in which UES5 requests a contiguous wide frequency band for broadband communications. Since the unused resources are fragmented, no frequency resource can be assigned to UES5 even though the total available capacity is sufficient to meet the demand. To have higher efficiency, each UES must be able to use fragmented frequency resources in the most flexible manner possible.

3. System concept

The concept of the DSDT system is shown in Fig. 2. On the Tx side, the DSDT adapter converts the output signal of the existing modem into a frequency-

domain signal by applying a fast Fourier transform (FFT) and divides it into multiple sub-spectra by using a spectrum dividing filter bank (Fig. 3(a)). The satellite assigns the divided sub-spectra to unused frequency resources and converts them into a single time-domain signal by applying an inverse FFT (IFFT).

On the Rx side, the DSDT adapter converts the received sub-spectra into the frequency domain by an FFT and re-shifts and combines all the sub-spectra by using its spectrum combining filter bank (Fig. 3(b)). It converts the combined signal into the time domain by an IFFT. The output signal of the DSDT adapter is demodulated by the existing modem.

4. Technical problem and novel approach

In the DSDT system, since received sub-spectra undergo independent phase offsets owing to the propagation delay, each Rx sub-spectrum undergoes phase distortion, as shown in Fig. 4(a).

In the Rx filter bank, sub-spectra k ($k=1, 2, \dots, n$, n : number of spectrum divisions), which are shifted by fs_k on the Tx side, are re-shifted by $-fs_k$ to regenerate the original signal. This frequency shift makes the phase characteristics of the regenerated signal become discontinuous, which invalidates the distortionless condition; consequently, the bit error rate (BER) performance is degraded, as shown in Fig. 4(b).

In addition, the DSDT system does not know the frame format of the existing modem because of its

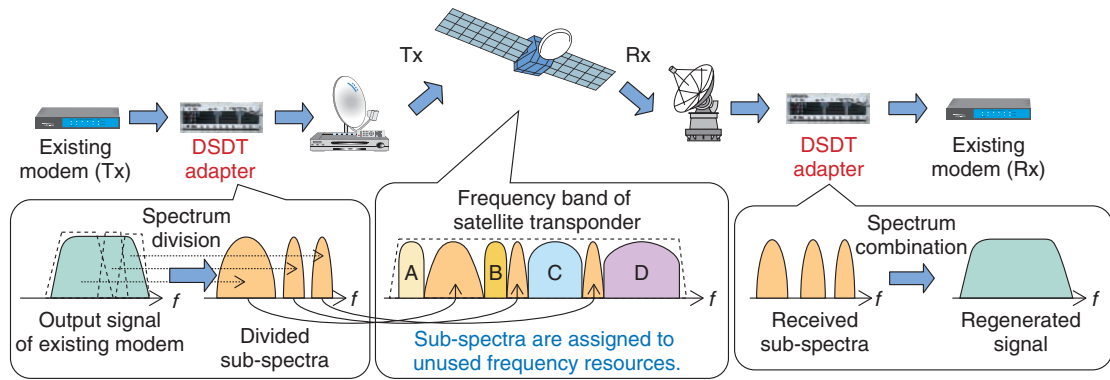


Fig. 2. Overview of DSDT system.

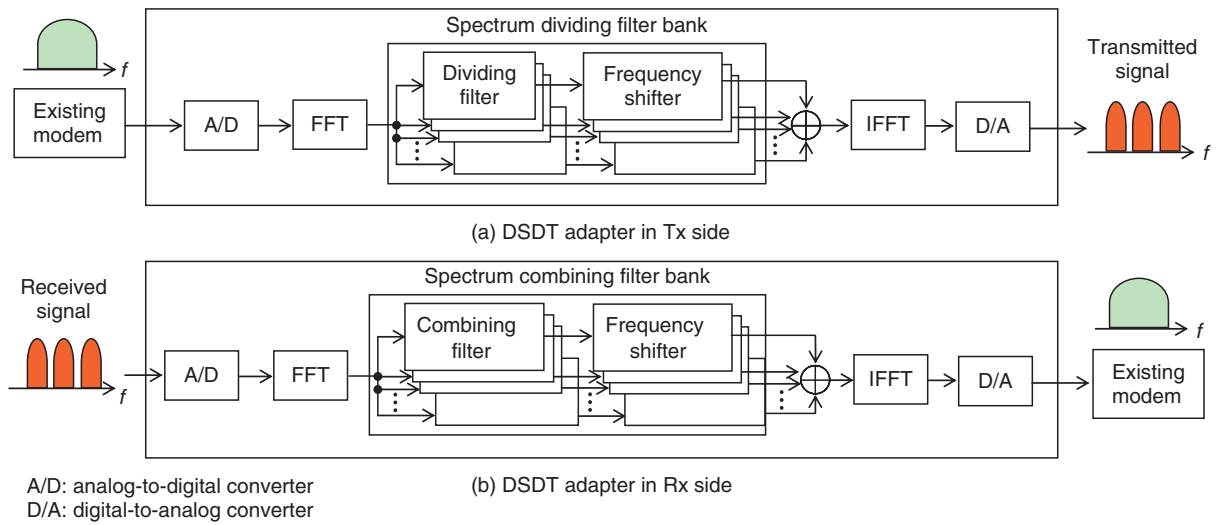


Fig. 3. Configuration of DSDT adapter.

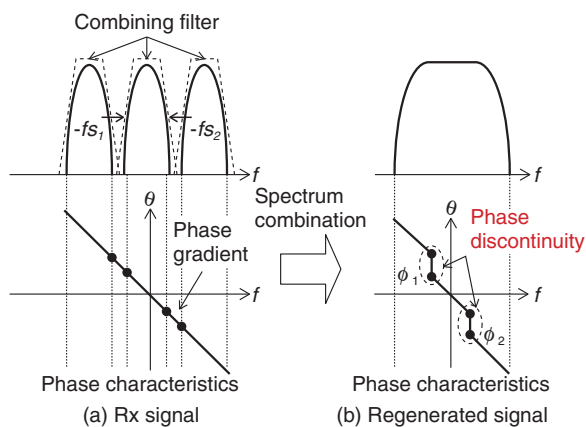


Fig. 4. Phase distortion after spectrum combination.

adapter-based design. Therefore, the phase distortion cannot be compensated for by using a specific frame pattern.

For phase distortion compensation, we use a blind phase compensation method (Fig. 5). Since the Rx-filtered and re-shifted sub-spectra undergo a phase shift due to the propagation delay, adjacent sub-spectra exhibit significant phase difference ϕ_k , as shown in Fig. 5(c). This compensation method estimates and compensates for ϕ_k for each pair of sub-spectra independently [4].

Since the blind phase compensation method estimates the phase compensation values regardless of the modulated signal spectrum patterns, no pilot signal or specific frame format is required.

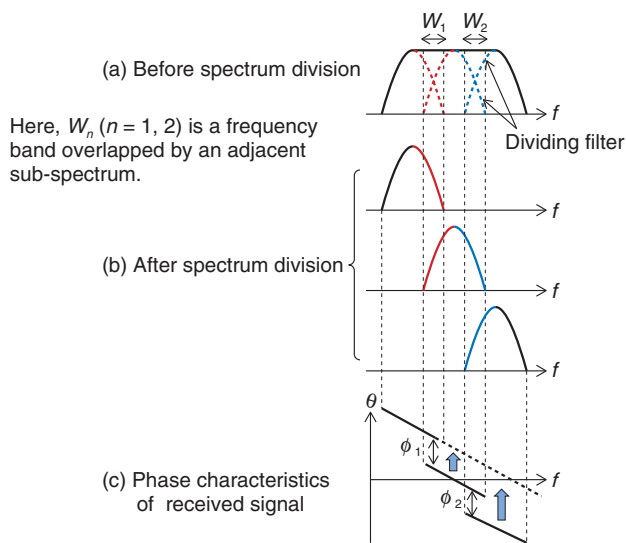


Fig. 5. Blind phase compensation method.

Table 1. Experimental parameters.

Modulation scheme	QPSK, 16QAM
FEC	LDPC code (code rate: 3/4)
Symbol rate	3.2 MHz
Sampling rate	25.6 MHz
Roll-off factor	0.25
Number of spectrum divisions (n)	No division, 2, 4, 8
FFT size	2048 points

16QAM: 16-state quadrature amplitude modulation
 FEC: forward error correction
 LDPC: low-density parity check
 QPSK: quadrature phase shift keying

5. Experimental evaluation

The performance of the DSDT system was evaluated in several experiments using a prototype DSDT adapter. As the existing satellite modem, we used Comtech EF Data CDM-625. The experimental parameters are shown in **Table 1** and the experimental configuration is shown in **Fig. 6**.

The output signal of the existing modem is shown in **Fig. 7(a)**. The DSDT adapter divided the signal into multiple sub-spectra, as shown in **Fig. 7(b)**. Received sub-spectra were combined and the original signal was regenerated by the combining filter bank, as shown in **Fig. 7(c)**. These observations confirm that the modulated signal was regenerated.

The quadrature phase shift keying (QPSK) constellations before and after phase compensation by the blind phase compensation method are shown in **Fig. 8**. The phase shift compensation was satisfactory. The BER performance is shown in **Fig. 9**, where the BER is plotted against the ratio of the energy per bit to noise power spectral density (E_b/N_0). For both of the modulation schemes tested, QPSK and 16-state quadrature amplitude modulation, the degradation in carrier-to-noise ratio was negligible compared with the undivided case.

These results demonstrate that the DSDT system can compensate for phase distortion satisfactorily and achieve flexible spectrum division.

6. Conclusion

This article described direct spectrum division transmission (DSDT) for satellite communications and an experimental evaluation of the DSDT system. Experiments on a prototype showed that the system's BER performance was close to that in the undivided case. Thus, we conclude that the DSDT system can divide the output signal of an existing modem flexibly and achieve high-capacity satellite communications.

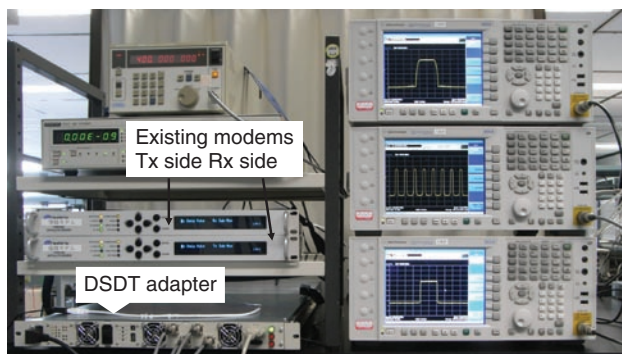


Fig. 6. Experimental system.

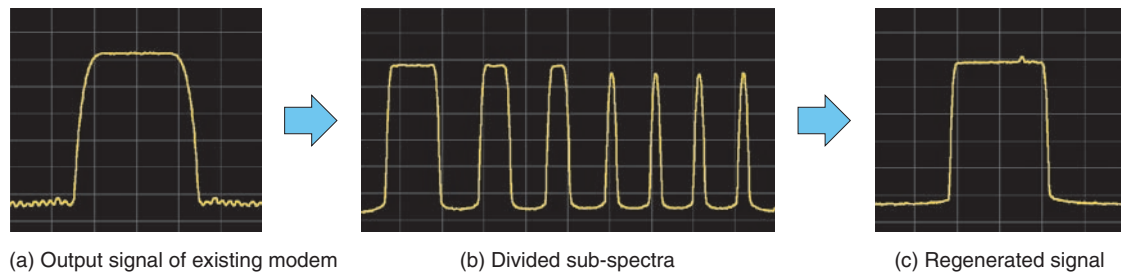


Fig. 7. Spectrum division and combination.

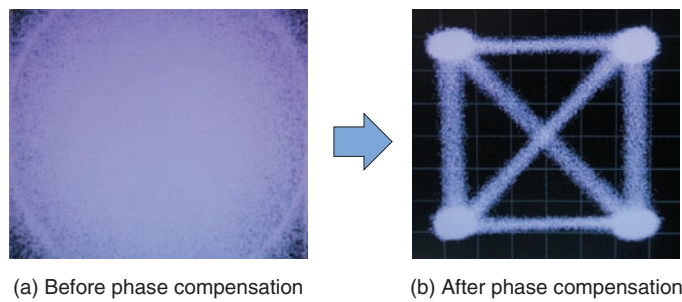


Fig. 8. Rx constellations.

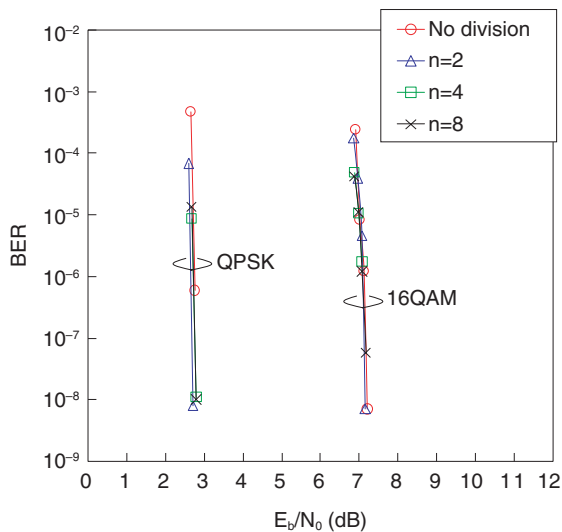


Fig. 9. Bit error rate performance.

through grants for “Research and Development on Dynamic Polarization and Frequency Control Technologies for High-capacity Satellite Communications”.

References

- [1] T. Hirose, K. Ohta, Y. Imaizumi, and H. Yoshida, “Satellite Communications Systems Used in Disaster Recovery Operations after the Great East Japan Earthquake and Tsunami,” IEICE Tech. Report, Vol. 111, No. 336, SAT2011-57, pp. 109–113, 2011.
- [2] J. Abe, F. Yamashita, K. Nakahira, and K. Kobayashi, “Direct Spectrum Division Transmission for Highly Efficient Frequency Utilization in Satellite Communications,” IEICE Trans. on Commun., Vol. E95-B, No. 2, pp. 563–571, 2012.
- [3] J. Abe, F. Yamashita, K. Nakahira, and K. Kobayashi, “Improving Frequency Utilization Efficiency of Existing Satellite Earth Stations with Bandwidth Decomposition Transmission Employing Spectrum Editing Technique,” IEICE Tech. Report, Vol., 111, No. 256, SAT2010-67, pp. 155–160, 2010 (accepted).
- [4] J. Abe, K. Nakahira, and K. Kobayashi, “A Blind Phase Compensation Method for Direct Spectrum Division Transmission,” Proc. of IEEE Global Telecommunications Conference (GLOBECOM 2011), Houston, Texas, USA.

Acknowledgments

This work is related to research sponsored by the Ministry of Internal Affairs and Communications

**Jun-ichi Abe**

Researcher, Satellite Communication Systems Group, Wireless Access Systems Project, NTT Access Network Service Systems Laboratories.

He received the B.E. degree in computer science and the M.E. degree in international development engineering from Tokyo Institute of Technology in 2004 and 2006, respectively. He joined NTT Access Network Service Systems Laboratories in 2006. He is currently working on modulation and demodulation schemes for next-generation satellite communication systems. He is a member of the Institute of Electronics, Information and Communication Engineers (IEICE).

**Katsuya Nakahira**

Research Engineer, Satellite Communication Systems Group, Wireless Access Systems Project, NTT Access Network Service Systems Laboratories.

He received the B.S. and M.S. degrees from Kochi University in 1989 and 1991, respectively. Since joining NTT Radio Communications Systems Laboratories in 1991, he has mainly been engaged in research on satellite communication network management and the development of satellite earth station equipment. His current interest is a channel allocation architecture for mobile satellite communication systems. He is a member of IEICE.

**Yoshinori Suzuki**

Research Engineer, Satellite Communication Systems Group, Wireless Access Systems Project, NTT Access Network Service Systems Laboratories.

He received the B.E., M.E., and Ph.D. degrees from Tohoku University, Miyagi, in 1993, 1995, and 2005, respectively. He joined NTT Wireless Systems Laboratories in 1995. Since then, he has been engaged in R&D of multibeam antenna feed systems for communication satellites. He is currently working on earth station antenna systems for mobile satellite communication systems. He received the Young Researcher's Award from IEICE in 2002 and the Best Paper Award of NTT Technical Publications in 2007. He is a member of IEICE.

**Takatoshi Sugiyama**

Senior Research Engineer, Supervisor, Group Leader, NTT Access Network Service Systems Laboratories.

Since joining NTT in 1989, he has been engaged in R&D of forward error correction, interference compensation, CDMA, modulation-demodulation, and MIMO-OFDM technologies for wireless communication systems such as satellite, wireless ATM, wireless LAN, and cellular systems.

4.6- μm -band Light Source for Greenhouse Gas Detection

Akio Tokura[†], Osamu Tadanaga, and Masaki Asobe

Abstract

This article describes a compact mid-infrared light source based on difference-frequency generation with a quasi-phase-matched LiNbO₃ waveguide for detecting N₂O gas. We obtained stable output power of 0.62 mW with an internal conversion efficiency of 5.9%/W for a 4.6- μm -band continuous-wave light source operating at room temperature. We demonstrated that this light source enables successful detection of N₂O gas at concentrations as low as 35 parts per billion. This light source is promising for highly sensitive in-situ continuous monitoring of N₂O, and it is also applicable to the detection of other greenhouse gases.

1. Introduction

Light sources in the mid-infrared (mid-IR) range are attractive for sensing trace gases. Many gases, including greenhouse gases (GHGs), exhibit strong absorption in the mid-IR range, especially from 2 μm to 5 μm , because their fundamental and rovibrational (coupled rotational and vibrational) modes are in this range [1]. The absorption intensities of such gases in the mid-IR range are higher than those in the near-IR range by a factor of 100 to 10,000. Therefore, mid-IR light sources have a strong advantage for highly sensitive and in-situ detection of GHGs.

For these applications, mid-IR light sources based on difference-frequency generation (DFG) in quasi-phase-matched (QPM) lithium niobate (LiNbO₃ (LN)) are promising because they can provide continuous-wave (CW) mid-IR light in the wavelength range from 2 μm to 5 μm and operate at room temperature. A high conversion efficiency can be achieved by using a waveguide structure, so we can obtain sufficient mid-IR output power [2]. With this structure, we have achieved high conversion efficiencies of 40%/W, 87%/W, and 100%/W for 3.2- μm , 2.7- μm , and 2.3- μm light sources, respectively [3]–[5].

In this article, we focus on the detection of nitrous oxide (N₂O), which is one of the major GHGs. N₂O

exhibits a strong greenhouse effect, even though its concentration in the atmosphere (322 parts per billion (ppb)) is low compared with carbon dioxide (385 parts per million (ppm)) and methane (1800 ppb). The atmospheric N₂O concentration has increased almost linearly at a rate of 0.8 ppb/year for decades. The most recent concentration measurement of 322 ppb in 2010 is about 19% higher than that in the pre-industrial era. Because N₂O has a long lifetime in the atmosphere, it will take a long time for its atmospheric concentration to fall. Furthermore, N₂O emissions in 2004 were 62.5% higher than in 1970 and accounted for 7.9% of the total anthropogenic GHG emissions in terms of carbon dioxide equivalents. Global annual emissions of anthropogenic GHGs from 1970 to 2004 are shown in **Fig. 1** [6]. To enable us to prevent increases in atmospheric N₂O concentration, we need to monitor N₂O emissions. A detection limit as low as a few tens of parts per billion is desirable for N₂O monitoring because the concentration of atmospheric N₂O is very low. Since N₂O gas exhibits its strongest absorption band in the 4.6- μm region, a 4.6- μm -band CW light source is suitable for in-situ continuous emission monitoring [1].

In this article, we describe a QPM-LN waveguide light source with a high conversion efficiency for N₂O gas detection. We introduce its operating principle and fabrication technique. We also present experimental results for N₂O detection with the light source and discuss the detection limit.

[†] NTT Photonics Laboratories
Atsugi-shi, 243-0198 Japan

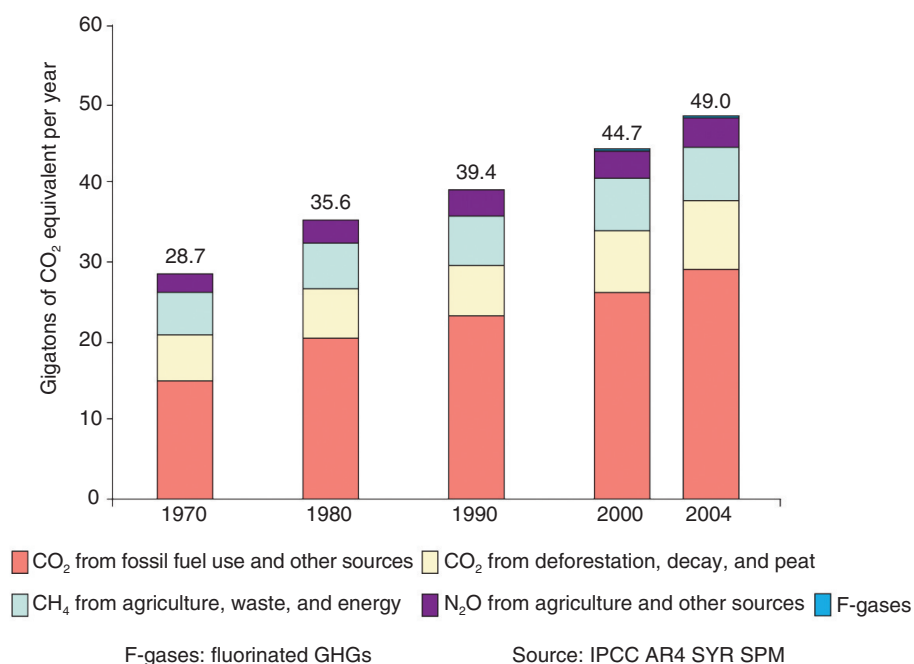


Fig. 1. Global annual emissions of anthropogenic GHGs from 1970 to 2004.

2. Principle of wavelength conversion

Mid-IR light in the 4.6- μm -band is generated by wavelength conversion based on DFG, which is a second-order nonlinear optical effect. For the DFG, a difference-frequency light, called the idler light, is generated from two input lights, which are called the pump and signal lights. When the pump light with wavelength $\lambda_p = c/v_p$ and the signal light with wavelength $\lambda_s = c/v_s$ are launched into a nonlinear optical crystal, the idler light with wavelength $\lambda_i = c/v_i$ ($v_i = v_p - v_s$) is generated by the DFG process, where c is the velocity of light and v is its frequency. This can be expressed using wavelength as

$$1/\lambda_i = 1/\lambda_p - 1/\lambda_s. \quad (1)$$

Various wavelength ranges of mid-IR light can be generated by choosing appropriate wavelength combinations of pump and signal lights from commercially available near-IR telecommunications laser diodes (LDs). To achieve efficient wavelength conversion from the interaction of the above-mentioned three waves, it is essential to satisfy the phase-matching condition. In most nonlinear crystals, this condition can be satisfied by only a limited number of combinations of wavelength and polarization. Quasi

phase matching relaxes the phase matching constraint and allows the wavelength conversion of arbitrary wavelength combinations. It is achieved by a periodically poled structure whose spontaneous polarization directions are reversed with period Λ with respect to the light propagation direction in the nonlinear crystal. This technique allows us to obtain conversions of various wavelength combinations simply by designing different poling periods. A DFG device using a QPM-LN waveguide is shown schematically in **Fig. 2**. Efficient wavelength conversion is achieved by satisfying the quasi-phase-matching condition ($\Delta\beta = 0$), where the phase mismatch $\Delta\beta$ is defined by

$$\Delta\beta = 2\pi[n_p/\lambda_p - n_s/\lambda_s - n_i/\lambda_i - 1/\Lambda]. \quad (2)$$

Here, n_p , n_s , and n_i are the refractive indices at the wavelengths of λ_p , λ_s , and λ_i , respectively. On the basis of a small signal approximation, where the attenuation of the two input light powers P_p and P_s is negligible, the converted light power P_i is given by

$$P_i = \eta P_p P_s / 100, \quad (3)$$

where η (%/W) represents the conversion efficiency and is given by

$$\eta = \eta_{\max} \text{sinc}^2[\Delta\beta L/2] \quad (4)$$

and

$$\eta_{\max} \propto L^2/A_{\text{eff}}. \quad (5)$$

The conversion efficiency η becomes constant ($\eta = \eta_{\max}$) when the phase mismatch is equal to zero. Therefore, the power of the converted light P_i increases in proportion to input powers P_p and P_s . Furthermore, P_i is proportional to the square of device length L and the inverse of effective interaction cross-section A_{eff} .

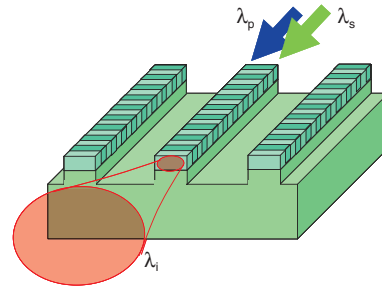


Fig. 2. Structure of QPM-LN waveguide device.

3. QPM-LN waveguide module

3.1 Waveguide fabrication

To reduce A_{eff} and thereby achieve efficient wavelength conversion, it is effective to use a waveguide structure because the three interacting lights are confined in a small core area. Our QPM-LN waveguide fabrication is based on direct bonding [7]. The fabrication process is shown in Fig. 3 [2]. We used Zn-doped LN as a core layer and lithium tantalate (LiTaO₃ (LT)) as a cladding layer. First, we made a periodically poled structure on an LN wafer by using a conventional electrical poling method. We then brought two wafers into contact in a clean atmosphere and annealed them at 500°C to achieve complete bonding. Next, the thickness of the core layer was reduced to around 10 μm by lapping and polishing. Then, the ridge structure was fabricated using a dicing saw. The waveguide was cut at an angle to prevent undesired back reflection. The Zn-doped LN core layer makes our waveguide highly resistant to damage. Moreover, because direct bonding does not use any adhesives, the fabricated waveguide is transparent in the mid-IR range and has better long-term reliability than ones made using adhesives.

3.2 Module design and DFG performance

The fabricated waveguide was assembled in a fiber pigtail module package. The module is 12 mm thick, 30 mm wide, and 73 mm long. To excite the transverse magnetic mode of the waveguide, we used a polarization-maintaining fiber as an input fiber. The module has a Peltier element and a thermistor to control the waveguide temperature. The phase-matching wavelength can be tuned by controlling the temperature. The pump and signal lights from the input fiber were coupled by a set of lenses to prevent heat damage to the connection area at high input power. This

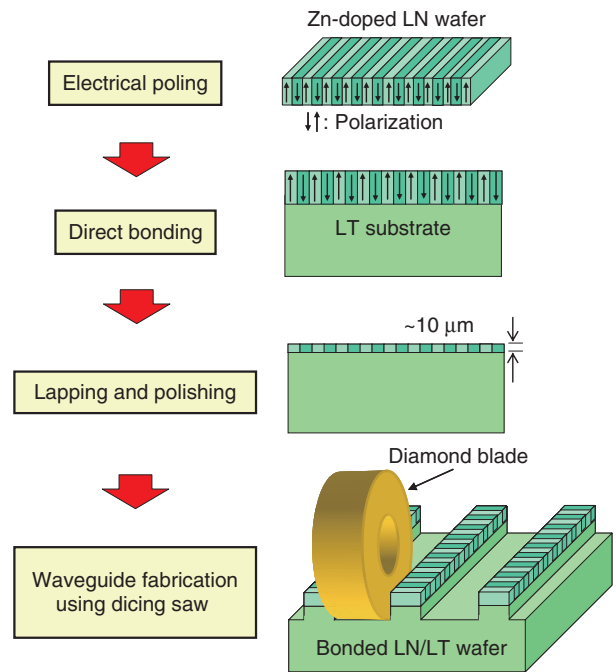


Fig. 3. Fabrication process of direct-bonded ridge waveguide.

enables us to inject 1.064-μm-band pump light of high power, which is amplified by an ytterbium-doped fiber amplifier (YDFA).

The DFG tuning curves at various LN waveguide temperatures as a function of signal wavelength when the pump wavelength was 1.06396 μm are shown in Fig. 4. The corresponding N₂O gas absorption lines calculated from values in the HITRAN (high-resolution transmission molecular absorption) database [1] are shown at the top of the graph. We could tune the phase-matching wavelength to a suitable absorption line for detection from among more than a dozen ones by controlling the waveguide temperature and the

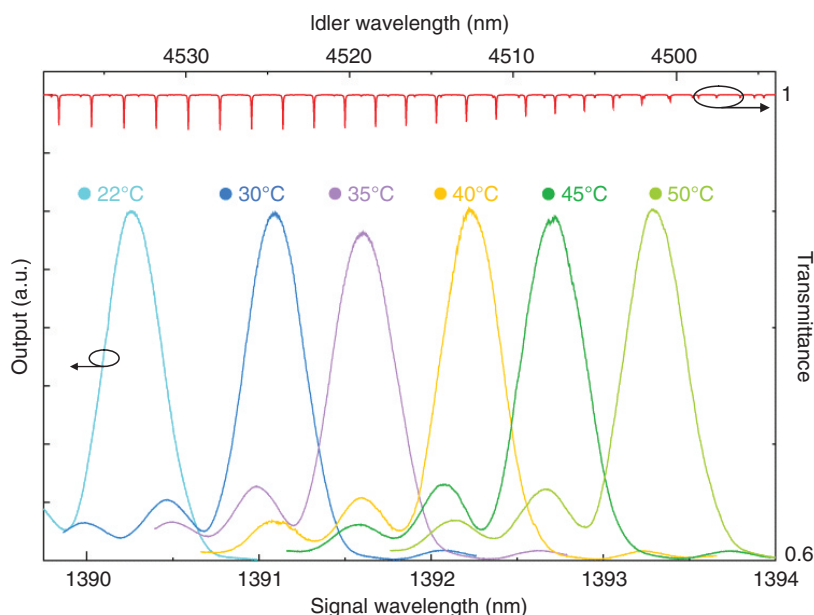


Fig. 4. DFG tuning curves at various LN waveguide temperatures.

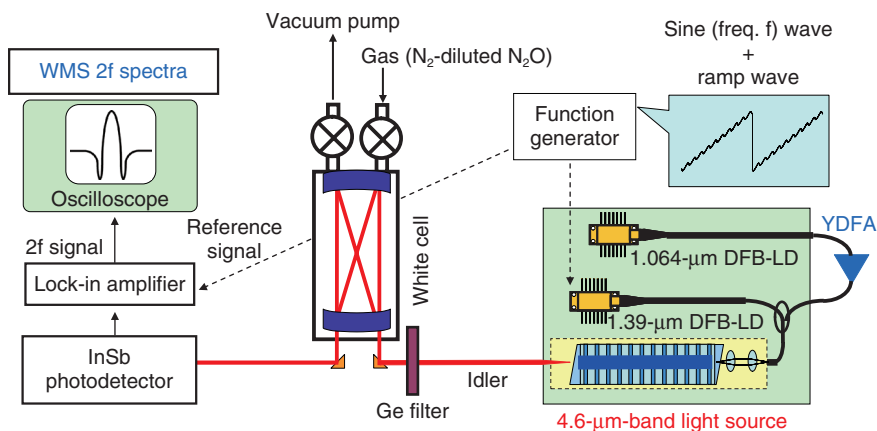


Fig. 5. Experimental setup for N_2O gas detection.

pump and signal wavelengths. We obtained CW mid-IR output with power of 0.62 mW at an internal conversion efficiency of 5.9%/W as typical properties when the pump and signal powers measured at the waveguide output side were 507 mW and 20.5 mW, respectively.

4. Light source and experimental setup

The experimental setup is shown schematically in Fig. 5. We fabricated a 4.6- μm -band light source for

detecting N_2O gas. The source is compact and reliable. It consists of two LDs, a YDFA, a wavelength division multiplexing fiber coupler, and a QPM-LN module. A 1.064- μm -band distributed feedback laser diode (DFB-LD) and a 1.39- μm band DFB-LD were used to generate the pump light and signal light, respectively. We used wavelength modulation spectroscopy (WMS) to obtain high sensitivity [8]. A 14-kHz sine wave superimposed on a 0.7-Hz ramp wave was generated by a function generator and injected as a forward current into the DFB-LD with a wavelength

of 1.39 μm . Current modulation of the signal light LD enabled us to obtain stable WMS spectra. The main component of the detection equipment was a White cell with a 16-m optical path. The sample gases were N_2 -diluted N_2O gas and N_2 -diluted air. The mid-IR light output from the cell was received by an InSb photodetector. We could align the output beam effectively by utilizing near-IR pump and signal outputs instead of the mid-IR output, which is difficult to visualize. The output signal from the photodetector was detected with a lock-in amplifier. The WMS spectrum consists of the second-harmonic ($2f$) component of the modulation frequency, which was derived from the lock-in amplifier.

5. N_2O detection using new light source

5.1 Absorption line of N_2O and detection technique comparison

Simulated optical transmittance results, which were calculated from HITRAN database values, for a pressure of 13.3 kPa and an optical path length of 10 m for atmospheric gases in the 4.6- μm -band range are shown in Fig. 6. Absorption lines from N_2O , water (H_2O), carbon monoxide (CO), and carbon dioxide (CO_2) can be seen. We selected the absorption line at 2201.75 cm^{-1} for N_2O measurement to avoid interference from the absorption lines of other gases. To obtain accurate values of gas concentration, it is preferable to perform N_2O measurement with the pressure reduced to 13.3 kPa because overlapping adjacent absorption lines are separated without any reduction in the absorption amount. We compared the WMS method with direct absorption measurement using the same absorption line at a gas concentration of 190 ppb. As shown in Fig. 7, the signal-to-noise ratio was improved by using the WMS method, and this allows us to achieve higher sensitivity.

5.2 N_2O WMS spectra and detection limit

The N_2O WMS $2f$ spectra at various N_2O concentrations are shown in Fig. 8. The input pump and signal powers were 200 mW and 40 mW, respectively. The red and blue lines are spectra at N_2O concentrations of 320 and 100 ppb, respectively. These spectra indicate that atmospheric N_2O concentration can be clearly detected and that N_2O concentrations lower than 100 ppb are detectable with this 4.6- μm -band light source.

To convert the WMS $2f$ signal into N_2O concentration, we used the WMS $2f$ peak value from the zero line. The WMS $2f$ peak intensities in the low-

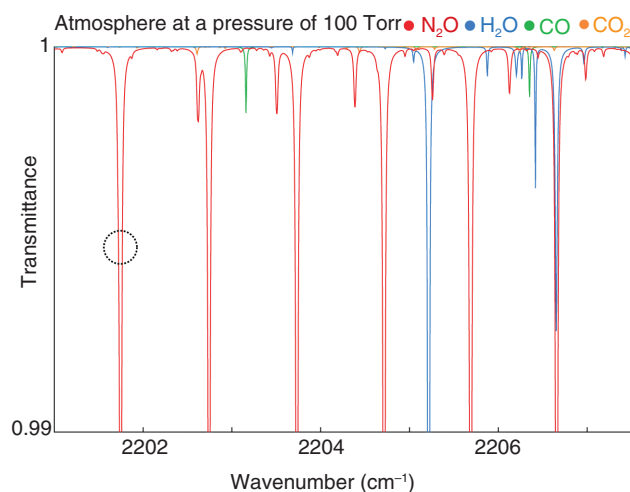


Fig. 6. Simulation results for optical transmittance of atmospheric gases.

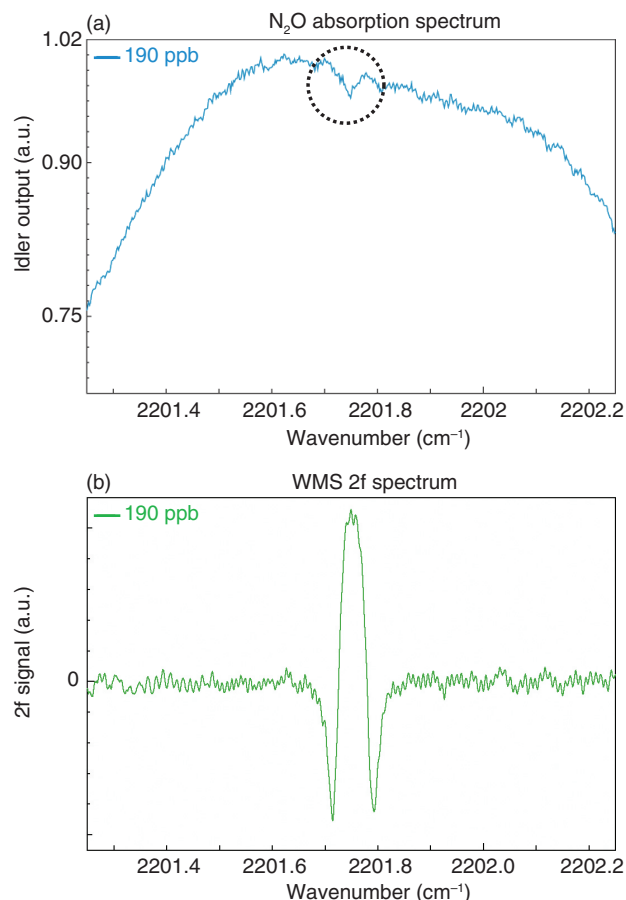


Fig. 7. Absorption spectra of (a) direct absorption method and (b) WMS method.

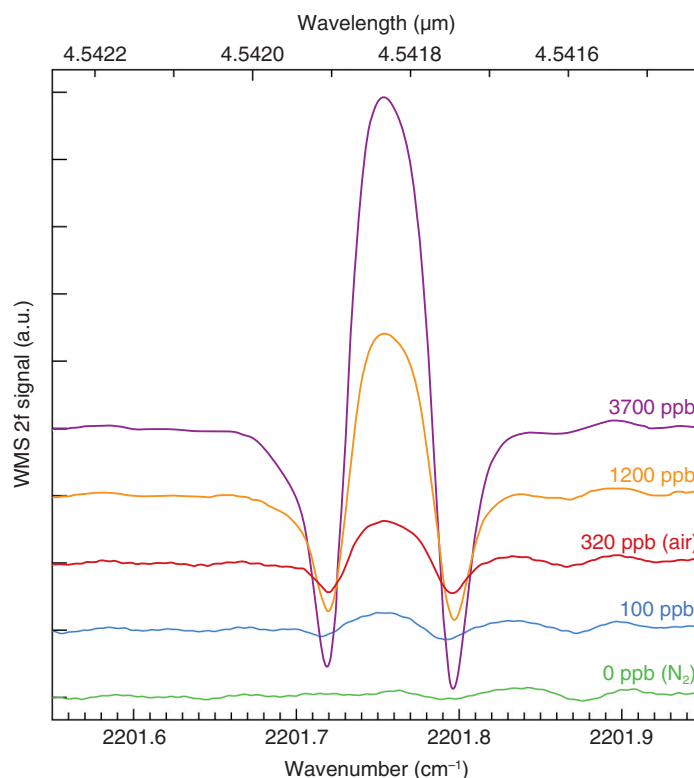


Fig. 8. WMS 2f spectra at various N_2O concentrations.

concentration range as a function of N_2O concentration are shown in Fig. 9. We defined the detection limit as the maximum noise level of measured spectra, which means that the limit is the concentration at which the signal-to-noise ratio is 1. The solid and broken lines in Fig. 9 correspond to the fitting curve and the maximum noise level, respectively. From the concentration at their crossing point, we found that the detection limit was 35 ppb, which corresponds to one-tenth of the atmospheric N_2O concentration. This result suggests that this light source is suitable for high-sensitivity in-situ monitoring of N_2O and is promising for monitoring other GHGs. The setup described above is also promising for N_2O measurements with a concentration resolution of around 100 ppb in the fields of agriculture and animal husbandry. Further improvements in sensitivity will be achieved by increasing the input pump power to 1 W and reducing the noise caused by the photodetector.

6. Conclusion

We have developed a 4.6- μm -band mid-IR light source based on DFG for N_2O gas detection. This is a

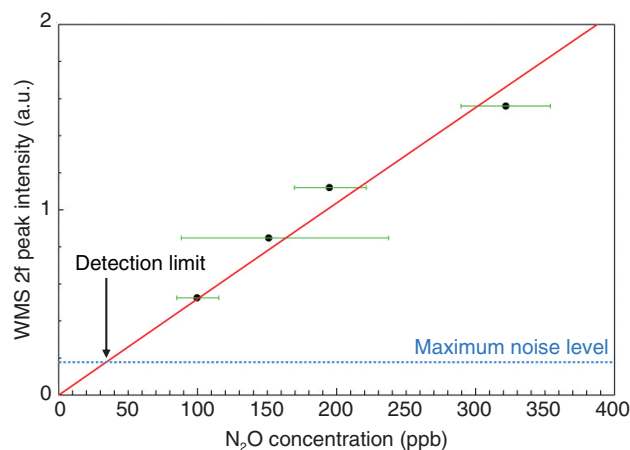


Fig. 9. WMS 2f peak intensities as a function of N_2O concentration.

reliable and compact light source that uses a QPM-LN waveguide module and two near-IR telecommunications LDs. We obtained stable CW output at a power of 0.62 mW and an internal conversion efficiency of 5.9%/W as typical properties. We successfully

demonstrated N₂O gas detection with this light source. The high sensitivity is attributed to lens coupling and to the WMS technique for detection. We obtained a detection limit of 35 ppb for N₂O detection. The DFG-based mid-IR light source using a QPM-LN waveguide can cover wavelengths up to about 5 μm, to which LN is transparent. This light source is promising for highly sensitive in-situ continuous monitoring of N₂O and other GHGs.

References

- [1] HITRAN database. <http://www.cfa.harvard.edu/hitran/>
- [2] O. Tadanaga, T. Yanagawa, and M. Asobe, "Mid-infrared Wavelength Conversion Laser for Highly Sensitive Gas Detection," *NTT Technical Review*, Vol. 7, No. 1, 2009. <https://www.ntt-review.jp/archive/ntttechnical.php?contents=ntr200901sf4.html>
- [3] O. Tadanaga, T. Yanagawa, Y. Nishida, H. Miyazawa, K. Magari, M. Asobe, and H. Suzuki, "Efficient 3-μm Difference Frequency Generation Using Direct-bonded Quasi-phase-matched LiNbO₃ Ridge Waveguide," *Appl. Phys. Lett.*, Vol. 88, pp. 061101-1–3, 2006.
- [4] O. Tadanaga, Y. Nishida, T. Yanagawa, H. Miyazawa, T. Umeki, K. Magari, M. Asobe, and H. Suzuki, "Efficient 2.7-μm Difference Frequency Generation Using Direct-bonded Quasi-phase-matched LiNbO₃ Ridge Waveguide and Investigation of O-H Absorption Influence," *Jpn. J. Appl. Phys.*, Vol. 46, No. 10A, pp. 6643–6646, 2007.
- [5] O. Tadanaga, T. Yanagawa, Y. Nishida, H. Miyazawa, K. Magari, M. Asobe, and H. Suzuki, "Widely Tunable and Highly Efficient 2.3-μm-band Difference Frequency Generation in Direct-bonded Quasi-phase-matched LiNbO₃ Ridge Waveguide," *Jpn. J. Appl. Phys. Pt. 2*, Vol. 45, No. 8, pp. L239–L241, 2006.
- [6] IPCC Fourth Assessment Report: Climate Change 2007 (AR4). http://www.ipcc.ch/publications_and_data/publications_and_data_reports.shtml
- [7] Y. Nishida, H. Miyazawa, M. Asobe, O. Tadanaga, and H. Suzuki, "Direct-bonded QPM-LN Ridge Waveguide with High Damage Resistance at Room Temperature," *Electron. Lett.*, Vol. 39, No. 7, pp. 609–611, 2003.
- [8] J. Reid and D. Labrie, "Second-harmonic Detection with Tunable Diode Lasers—Comparison of Experiment and Theory," *Appl. Phys. B*, Vol. B26, No. 3, pp. 203–210, 1981.



Akio Tokura

Researcher, Advanced Opto-electronics Laboratory, NTT Photonics Laboratories.

He received the B.E. and M.E. degrees in physics from Tokyo Institute of Technology in 2001 and 2003, respectively. He joined NTT Basic Research Laboratories in 2003 and studied the physical and chemical properties of carbon nanotubes and carbon nanotube growth. Since 2010, he has been engaged in research on nonlinear optical devices, including wavelength converters and their spectroscopic applications, in NTT Photonics Laboratories. He is a member of the Japan Society of Applied Physics (JSAP).



Osamu Tadanaga

Senior Engineer, Photonic Technology Development Center, NTT Electronics.

He received the B.E. and M.E. degrees in materials science and engineering from Kyoto University in 1993 and 1995, respectively, and the Ph.D. degree in the area of nonlinear optics from the University of Tokyo in 2009. Since joining NTT in 1995, he had been engaged in research on surface-normal modulators, VCSELs, and quasi-phase-matched LiNbO₃ wavelength converters. After the work described in this article, he moved to NTT Electronics in 2010. He is a member of JSAP, the Optical Society of Japan, and the Institute of Electronics, Information, and Communication Engineers (IEICE).



Masaki Asobe

Senior Research Engineer, Supervisor, Group Leader, Innovative Photonic Core Technology Research Group, NTT Photonics Laboratories.

He received the B.S. and M.S. degrees in instrumentation engineering from Keio University, Kanagawa, in 1987 and 1989, respectively. He received the Ph.D. degree for work in nonlinear optics from the same university in 1995. In 1989, he joined NTT Laboratories, Kanagawa, Japan, where he has been engaged in research on nonlinear optical devices, such as ultrafast all-optical switches and broadband wavelength converters, and high-speed optical communications systems. He is a member of JSAP, IEICE, and the Optical Society.

Jubatus: Scalable Distributed Processing Framework for Realtime Analysis of Big Data

Satoshi Oda, Kota Uenishi, and Shingo Kinoshita[†]

Abstract

This article describes a distributed machine learning framework called Jubatus for deep realtime analysis of big data that we are jointly developing with Preferred Infrastructure Corporation. The main challenge for Jubatus is to achieve scalable distributed computing for profound analytical processing such as online machine learning algorithms and provide a common framework for different supported algorithms. After giving an overview of Jubatus, this article focuses on a key mechanism called *mix*, which is a new synchronization method among servers to scale out online machine learning algorithms, which are potentially difficult to distribute and parallelize. It synchronizes servers loosely and has a relaxed consistency to the extent allowed by the performance and learning accuracy requirements. This article also evaluates performances such as throughput and scalability and verifies the degree to which the consistency requirement is relaxed.

1. Introduction

With large quantities of data of various types being produced, distributed, and shared around the world, it is becoming increasingly important for businesses worldwide to acquire new knowledge from data such as people's behaviors, system operational logs, and environmental information obtained through their business activities. This huge amount of data is known as *big data*. Much of it is unstructured data that is not stored in databases, and in the past it was too large to analyze and was therefore discarded. However, the analysis of big data at a low cost has recently been facilitated by open-source software systems such as Hadoop [1], which allow distributed computing across clusters of inexpensive commodity computers. This has made it possible to perform analysis within realistic time limits and obtain useful insight from the analysis.

This kind of analytical processing is based on batch processing in which data has been temporarily stored

and processed as a batch. As analytical methods, it utilizes statistical analysis, such as summation, and machine learning. In addition, a machine learning library called Mahout running on Hadoop has been developed; it enables batch-type sophisticated analysis of big data in a scalable manner. There is increasing need for realtime capabilities, prompted by demonstrations of the validity of such large-scale data analysis [2].

One of the technologies with realtime capabilities is online stream-processing. It supports push-type analysis methods in which analysis results are calculated incrementally as soon as data arrives without the data being stored in a database, instead of the conventional pull-type analysis performed on a database after data has been stored. Representative examples of such online stream-processing systems are IBM InfoSphere Streams, Oracle CEP, StreamBase, Sybase Event Stream Processor, and Truviso. Each of these is a commercial product with a full lineup of capabilities, functions, development environments, and operating tools. They are already in use, including use in mission-critical areas such as finance, communications, the military, and medicine. However,

[†] NTT Software Innovation Center
Musashino-shi, 180-8585 Japan

these deployments are based on the assumption that scaling up requires expensive hardware and they do not support sophisticated analysis functions such as machine learning but only simple statistical functions.

Therefore, for further business success, it is becoming more important to enable more sophisticated and timely analysis of big data at a low cost. For this, the key challenge is to create a scalable distributed computing framework across clusters of inexpensive commodity computers for realtime and profound analytical processing using online machine learning algorithms.

2. Jubatus

To address this challenge, NTT Software Innovation Center and Preferred Infrastructure Corporation have cooperated in the development of Jubatus [3], [4] since 2011. Jubatus is a distributed computing framework for realtime and profound analytical processing using online machine learning algorithms, rather than the batch processing provided by Mahout/Hadoop and the simple statistics processing provided by online stream-processing systems. It has scale-up capability whereby the performance of the system increases linearly with the addition of inexpensive commodity computers.

To achieve this scalability, Jubatus must distribute online machine learning processing among many computers and synchronize their learning results. An iterative parameter mixture [5], [6] has been found to be effective as an algorithm for the synchronization of this distributed processing [7]. Jubatus has been modified to use this algorithm to achieve realtime processing.

Among various types of online stream-processing, two types of machine learning—linear classification and linear regression—were initially implemented for Jubatus because they are basic analytical functions and have a much broader range of applications. To support these types of machine learning, Jubatus is aimed at stateful stream-processing, where the status of a stream-processing node can be updated in accordance with the content of arriving data. To enable application programs to be developed more efficiently, Jubatus supports a full range of feature conversion functions that facilitate the conversion of unstructured data into a format that can be used in machine learning [8].

2.1 Current position and roadmap

Jubatus is intended to be a framework for realtime analytical processing. However, the initial version applies only a few online machine learning algorithms, such as linear classification and regression algorithms, to the distributed computing environment by using an iterative parameter mixture, so it is not yet ready to be provided as a full-range framework. This is because, although machine learning is generally taken to be a problem of numerical optimization, it is not obvious how to design generic forms that will enable distributed processing, in other words, frameworks.

In the future, the challenge of designing a suitable framework will be to extract generic calculation models in a similar way to MapReduce by applying more machine learning algorithms and prototyping applications aimed at real-life tasks.

2.2 Distributed processing

2.2.1 Overview

Jubatus basically achieves realtime analysis of a huge amount of data that cannot be processed by a single server by distributing the data over multiple servers. In machine learning, there are two types of processing: training and prediction. In the training process, the model data is updated by a machine learning algorithm such as a passive-aggressive (PA) algorithm using supervised data. In the prediction process, data that a server has received is processed using the model data and this enables the prediction to be performed. For example, in the case of classification algorithms, the input data is predictively classified into several specified groups on the basis of the model data.

In the training process, all the servers involved in the distributed processing initially have the same model data, but the model data varies as the individual training proceeds. With an iterative parameter mixture, if training is done with a given amount of data at each server, the model data of all servers is integrated into a new set of model data. This new model data is shared among servers again and each server then performs training individually.

As Jubatus is based on online processing, the servers collaborate in synchronizing the model data when either of the following conditions is satisfied: any one server has trained a given number of data items or a specific given time has elapsed. This synchronization *mix* enables training results to be shared while all the servers are performing the training in parallel. Since the training and prediction traffic is distributed to

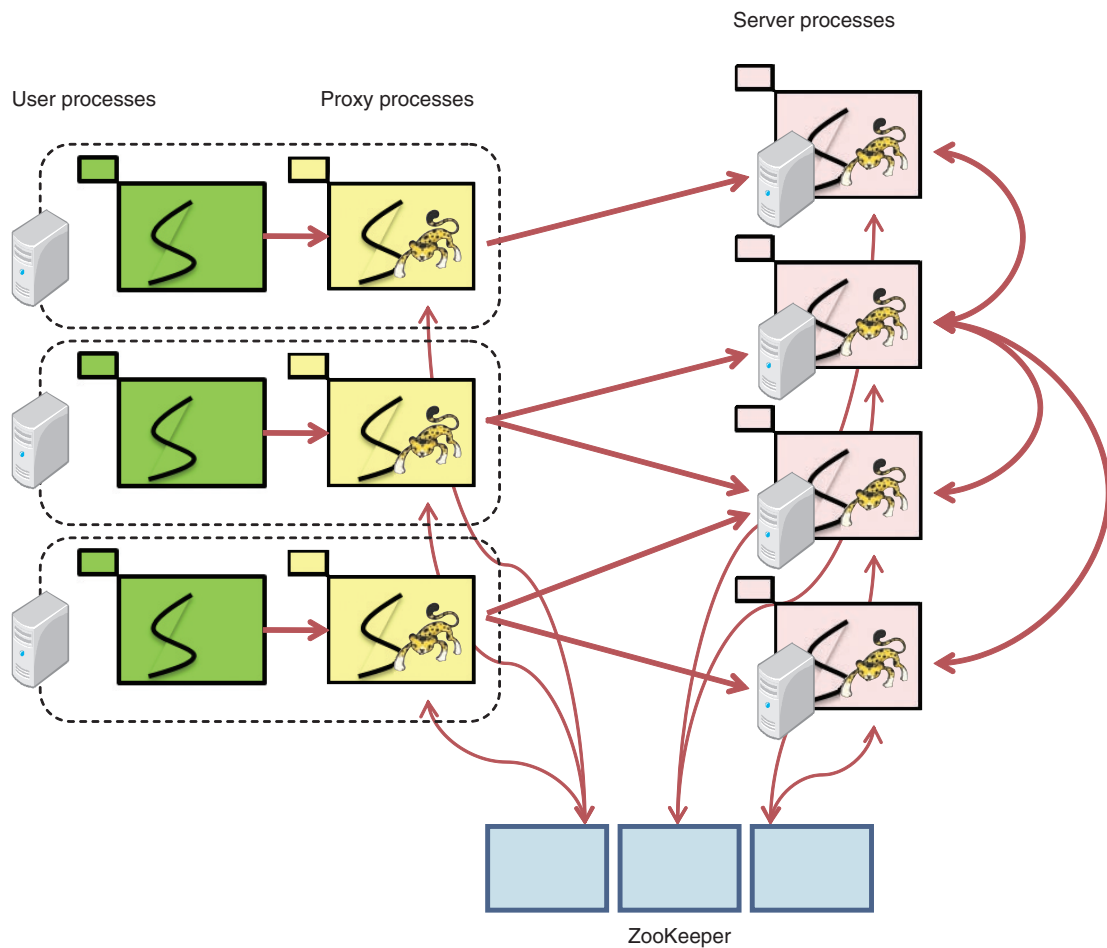


Fig. 1. System architecture of Jubatus.

individual servers, it is possible to scale the throughput in accordance with the number of servers and the amount of calculation resources, while maintaining the response time. The distributed processing architecture of Jubatus is discussed below.

2.2.2 Basic architecture and membership management

The Jubatus system consists of server processes that perform feature conversion and machine learning processing (training and prediction), proxy processes that allocate requests from clients to servers, ZooKeeper* [9] processes, and user processes that clients have assembled, as shown in Fig. 1. Note that if there is only one server process, a user process can access it directly without going through a proxy process.

A server process, with the name `jubaclassifier` or `jubaregression` in the Jubatus system, maintains

model data and performs the training and prediction processing. The system implements horizontal scalability in response to the load by deploying a number of these server processes. Each server process registers its own identity (ID), e.g., its Internet protocol (IP) address and listening port number, in ZooKeeper. ZooKeeper exchanges KeepAlive messages with the server processes at regular intervals. If a server process stops for some reason, such as a hardware failure, ZooKeeper detects that and automatically deletes its registered ID.

A user process is a process executed by a user program of Jubatus. It may collect data from other systems, request server processes to train and predict the data, and receive the prediction results. When the user process is used by a web application, it is assumed to be a web server process such as Apache.

A proxy process, called `jubakeeper` in the Jubatus system, relays communications transparently from a

* ZooKeeper is a trademark of The Apache Software Foundation.

user process to a server process. It receives a request from a client, selects a suitable server from the list of IDs registered in ZooKeeper, and transfers the request to that server. The client can therefore execute the request without being aware of either the server process that is operating or any increase or decrease in the number of server processes.

Since the remote procedure calls of Jubatus are performed by synchronous communications, an environment is created in which the best performance occurs when the total number of user process threads is greater than the total number of proxy process threads, which is greater than the total number of server process threads.

While enabling scale-out, this distributed configuration also ensures that even if part of an individual process is stopped, the performance (and precision, in some cases) will deteriorate temporarily, but the overall system will not halt; thus, this configuration corresponds to a distributed system with no single point of failure.

2.3 Synchronization method: *mix*

Jubatus has an extension of the iterative parameter mixture, which is called *mix*. This concept is unique to Jubatus. An iterative parameter mixture is a method of machine learning in which all of the model data trained in the servers is collected together and averaged and then shared again for further training. This is regarded as a problem of replication when data updated by an individual server is synchronized by all of the servers. In other words, from the data management viewpoint, the training, average calculations, and predictions in machine learning are equivalent to the updating, synchronization, and reading of data, respectively.

In an ordinary database system, the traditional requirement is to satisfy *atomicity, consistency, isolation, and durability* (ACID) [10]. In other words, updated data is always synchronized, even in a distributed environment, and reading must be enabled from the instant that the update was successful. However, it is difficult to implement a distributed data management system that satisfies strict ACID properties because of the constraint called the CAP theorem (C: consistency, A: availability, P: partition tolerance) [11]. Recent distributed storage techniques have been able to implement practicable performance in a range in which this constraint is satisfied. They achieve this by defining a behavior called *basically available, soft state, eventually consistent* (BASE), in which mainly the consistency (C) part of the constraint is relaxed.

In BASE, it is sufficient to have matching databases in which all of the data updates are eventually implemented. This consistency model is called Eventual Consistency [12].

In the field of numerical optimization problems such as statistical machine learning, deterioration in the consistency of data synchronization is considered to be a loss of data to be trained, and it results in a decrease in accuracy. Conversely, by applying the scale-out approach, which enables a large amount of data to be processed in parallel, it is possible to use enough training data to overcome that loss and preserve realistic accuracy while increasing performance. Focusing on this point, we devised a data synchronous algorithm called *mix* which is of a form that has an even more relaxed consistency requirement. The *mix* in linear classifiers currently implemented in Jubatus is described below.

With an iterative parameter mixture, once training with a given quantity of data is complete, the system calculates the average of the model data in all of the servers and uses it as an initial value for model data in the next phase of the training. In other words, each phase is partitioned in accordance with the data size.

With Jubatus, servers do not necessarily all process equal amounts of training data, so each phase is partitioned by either data quantity or time, as mentioned in section 2.2.1. Each phase ends when any of the conditions has been satisfied, and the *mix* starts. More specifically, the sequence (shown in Fig. 2) is as follows.

- (1) The server process that started the *mix* acquires a lock on ZooKeeper and becomes the master.
- (2) It acquires the server process list from ZooKeeper and receives model data that will become the subject of the *mix* from all the processes.
- (3) It performs synchronization, e.g., calculates the average, with respect to the received data.
- (4) It distributes the synchronized data to all the processes.
- (5) Each server process updates its own model data with the synchronized data.
- (6) The master that has confirmed the update releases the lock on ZooKeeper.

In the case of a batch-type iterative parameter mixture, there would be no loss of training data because no training is done during steps (2) to (5), but with the Jubatus *mix*, training is performed during this time. This is because Jubatus is designed to increase accuracy during this time because it supports online-type realtime processing in which training and prediction requests arrive continuously during the time and must

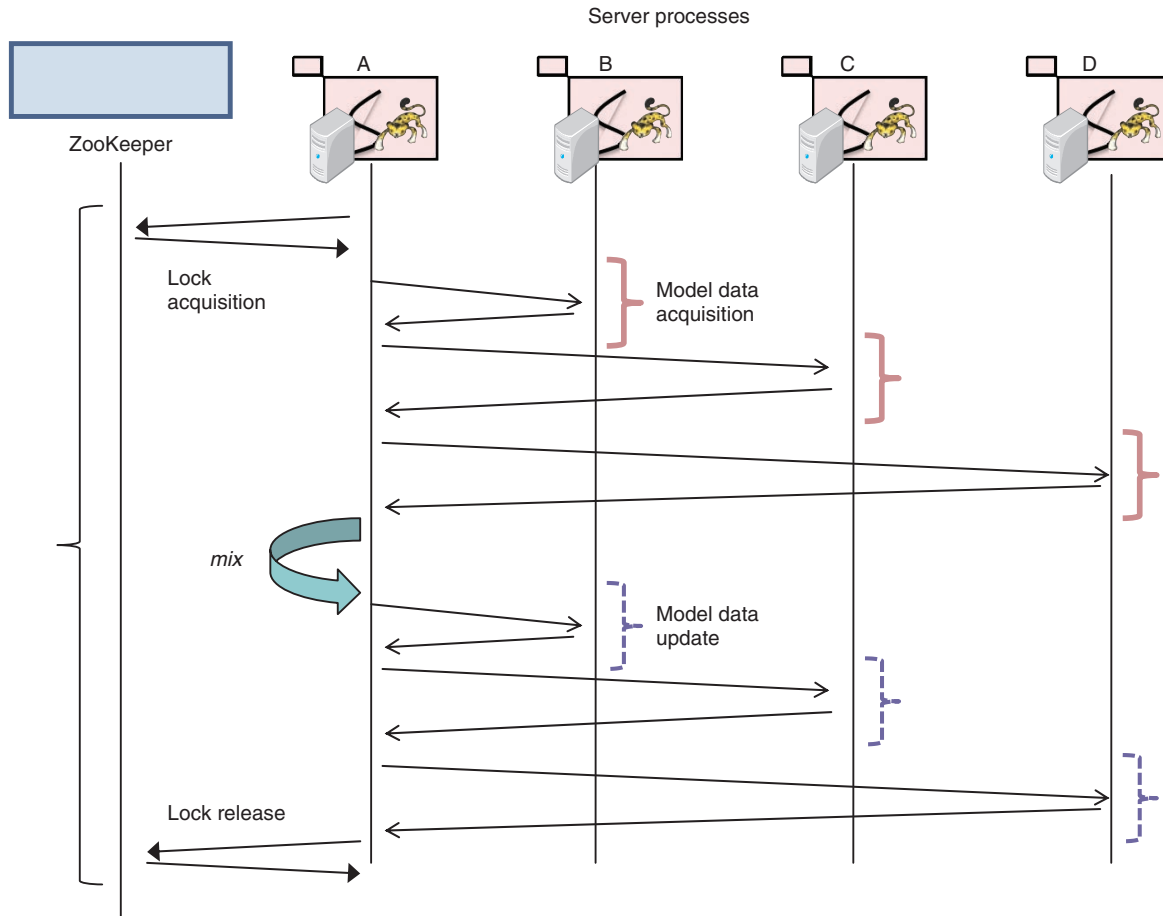


Fig. 2. Sequence of *mix*.

be responded to in real time.

Jubatus also provides a further advantage: it is simple to create a configuration in which, if the master process should fail during this time, so that the *mix* processing is interrupted, the status is handed over to another master that starts a new *mix*. The individual training results of each server obtained during steps (2) to (5) are updated with the synchronized model data received in step (5), so they are not reflected in subsequent model data. Note that it might be possible to reflect the training results during steps (2) to (5) by buffering them and retraining or remixing.

In previous research [8], we demonstrated that it is possible to implement linear scalability and a timely response with high training accuracy by means of a simple *mix* operation that permits such training data losses. We have also demonstrated that the effect on accuracy was limited when certain real data was used and indeed there have been no problems in actual

use.

The present article, on the basis of experiments, further generalizes this situation and clarifies the data training performance and its behavior in distributed processing by Jubatus using *mix*.

3. Applicable algorithms

Jubatus implements several online machine learning algorithms, such as a linear classification algorithm (classifier), linear regression algorithm (regression), and nearest neighbor search algorithm, in addition to basic statistics functions. Among them, this article describes a linear classification algorithm (classifier) and linear regression algorithm (regression) as machine learning algorithms, and an iterative parameter mixture in the algorithms to make both algorithms correspond to distributed processing.

3.1 Classifier

The linear classification problem is the problem of predicting $y \in \{+1, -1\}$ according to whether a feature vector $\phi(x) \in R^m$ corresponding to an input x belongs to a certain class C . Jubatus implements five perceptrons: PA [13], PA2, PA3, CW, and ARROW.

3.2 Regression

The regression problem is the problem of assigning a real-valued output $y \in R$ for a feature vector $\phi(x) \in R^m$ corresponding to an input x . Jubatus implements a linear regression model using PA. With a linear regression model, we use the parameter $w \in R^m$ and forecast by means of $\hat{y} = w^T \phi(x) \in R$ with respect to input x .

3.3 Iterative parameter mixture

As mentioned in section 2.3, the iterative parameter mixture is used in the synchronization of training results, i.e., model data. The iterative parameter mixture for the PA algorithm, which is used by classifiers and regressions, is presented in this section, and a generic case of the *mix* that we assume to be installed in Jubatus is also demonstrated. In a certain phase τ , assume that the model data retained by a server i (where $i = 1, \dots, N$) is $w_i(\tau)$ and that the model data trained using supervised data obtained after the previous *mix* is $w'_i(\tau)$. The iterative parameter mixture in PA is expressed by the cumulative average:

$$w(\tau+1) = \frac{1}{N} \sum_{i=1 \dots N} w'_i(\tau).$$

With a linear classifier implementation in Jubatus, the model data w is a vector with few enough dimensions for storage in physical memory; sending all of the w_i data over the network and calculating averages would be unrealistic in practice. Therefore, only differences that accumulate during each *mix* are transferred over the network to synchronize w , as shown in the following equations.

$$w_i(\tau+1) = w_i(\tau) + \Delta w(\tau) \quad (1)$$

$$\Delta w(\tau) = \frac{1}{N} \sum_{i=1 \dots N} \Delta w'_i(\tau) \quad (2)$$

The only data transferred over the network is $\Delta w'_i(\tau)$ and $\Delta w(\tau)$. Each of these is limited to at most a quantity equivalent to the number of feature quantities obtained by the training after the previous *mix*. Note that the model data used during actual training and classification is given by

$$w = w_i(\tau) + \Delta w'_i(\tau)$$

and this calculation is done as required. This format is similar to linear regression.

4. Experiments

The precision and performance of machine learning are strongly dependent on the dataset. For that reason, these experiments evaluated the number of pieces of supervised data that were trained per unit time (throughput), with the data dimensions being fixed. Machine learning has a computing part in which the central processing unit (CPU) is a bottleneck and a data update part in which memory access is a bottleneck. In addition to these, Jubatus also has bottlenecks on the network side because it is based on the client/server model. We provided sufficient numbers of client and proxy processes, 16 threads \times 4 machines each, to ensure that network-related bottlenecks could be ignored, and we evaluated the server-side performance.

Random data with specified data dimensions was generated and used as a training dataset. More specifically, if we assume that the supervised data is (label, datum) and that the number of dimensions of a datum is N , we obtain data for which label $\leftarrow \{0, 1\}R$ and datum $= [0, 1]_i$, where $i = 1, 2, \dots, N$. Since there is no correlation between label and datum, the throughput level is lower than for a dataset of real data of the same magnitude. Since this dataset is random data generated from a uniformly random distribution, the data could be very dense in contrast to the dataset of sparse vectors assumed by Jubatus. Therefore, with this dataset, memory bottlenecks can readily occur, so the time required by the *mix* could be high.

4.1 Experiments in a single-server environment

A Jubatus server can initiate a number of threads with a single process. First, the throughput of a single thread was evaluated. The CPU of the server used in the experiments was a Xeon X3430 2.4 GHz (4 CPUs, 4 cores). Results for $N = 32, 64, 128, 256, 512$, and 1024 are shown in **Fig. 3**.

This figure shows that the numbers of dimensions and the numbers of queries per second (qps) are substantially inversely proportional to each other. (Memory or CPU creates a bottleneck.) We can also see that there is no great difference between classifier and regression.

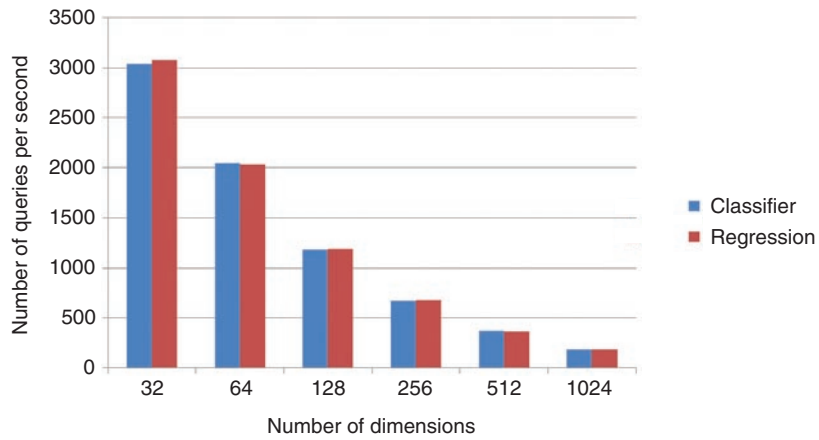


Fig. 3. Relationships between the number of dimensions and the number of queries per second with a single thread.

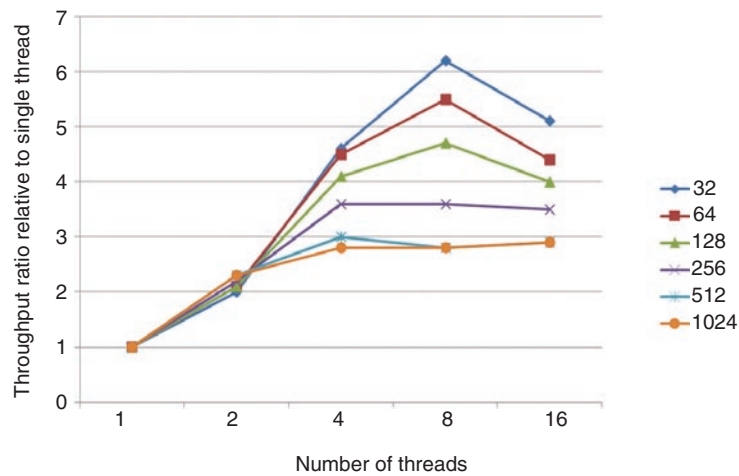


Fig. 4. Training throughput with single server.

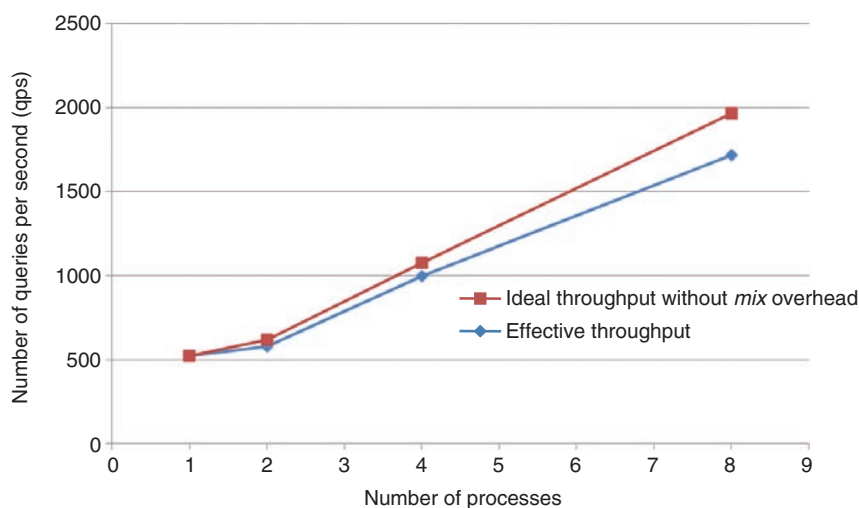
Second, changes in throughput when the number of threads was increased were evaluated. The number of server threads, assuming qps to be 1 when there is one thread, is plotted on the horizontal axis of the graph in **Fig. 4** and the relative qps is plotted on the vertical axis. Since the computer has 16 cores installed, which is at least the maximum number of threads, a graph of $x = y$ should be drawn when the bottleneck is caused by the CPU rather than by memory.

It is clear that performance reaches a maximum when the number of threads is between 4 and 8, depending on the number of dimensions, and performance is lower for 16 threads. The bottleneck at 8 or 16 threads may be caused by memory: too many

threads could result in slow throughput because of memory lock and unlock overheads in general. This means that increasing the number of CPUs and the number of cores in the single-server environment will cause a scale-up limit in this vicinity.

4.2 Experiments in a distributed environment

We evaluated the throughput of Jubatus in a distributed server environment using the *mix* process. In the light of the evaluation described in section 2.3, we performed evaluations with a configuration in which the number of threads was 8 and $N = 1024$. The *mix* timing was when 16 s had elapsed or when 512 instances of training had been performed in the initial



Number of processes, threads	Ideal throughput without <i>mix</i> overhead (qps)	Drop rate by <i>mix</i> process (%)	Effective throughput (qps)
1, 8	521	0	521
2, 16	620	6.6	579
4, 32	1076	7.2	999
8, 64	1967	12.7	1717

Fig. 5. Numbers of processes and training throughput.

setting of Jubatus. Since the quantity of arriving data was sufficiently large in this experimental environment, the number of instances of training data was taken as the trigger for *mix*. As introduced in section 4.1, training data is lost during the *mix* processing between the sending of differences and the receiving of synchronized data. The number of pieces of data (data items) being trained by each server during the *mix* process was evaluated (the number of data items that dropped out). Effective throughput, i.e., the actual number of training data items, was calculated by subtracting the number of lost data items from the total number of trained data items.

The experimental results are shown in **Fig. 5**. The throughput increased linearly with the number of servers because more than enough proxy processes were provided. Since the time required for the *mix* process also increased as the number of servers increased, the proportion of supervised data that was not reflected in the training results also increased as a consequence. However, the number of pieces of trained data per unit time in the entire system increased substantially as the number of servers increased. Note that the throughput for two nodes does not increase proportionally, in contrast to that for one node, owing to the overhead of a proxy pro-

cess, which is unnecessary for the single-node configuration.

5. Conclusions and future challenges

This article has introduced Jubatus, a distributed computing framework for realtime analysis of big data. In particular, it described *mix*, which is a key method of Jubatus. *Mix* performs asynchronously with respect to the training of the entire system by an iterative parameter mixture in online classification and online regression problems in a distributed environment. We also evaluated the performance of the training process in both a single-server environment and a distributed server environment in a version of Jubatus implementing the *mix* method and confirmed its scalability.

Experiments in a distributed environment with eight nodes utilizing the *mix* demonstrated that there was an overall loss of 12.7% of the training data, but the number of items of training data per unit time increased in a substantially linear manner. This characteristic will be useful when statistical machine learning is applied to large quantities of data.

Future work includes supporting more machine learning algorithms, such as graph mining and

clustering, and confirming that the calculation framework based on a *mix* that is a generalized iterative parameter mixture will be valid for other machine learning algorithms and analysis tasks.

References

- [1] Apache Hadoop. <http://hadoop.apache.org/>
- [2] D. Borthakur, J. Gray, J. S. Sarma, K. Muthukkaruppan, N. Spiegelberg, H. Kuang, K. Ranganathan, D. Molkov, A. Menon, S. Rash, R. Schmidt, and A. Aiyer, "Apache Hadoop Goes Realtime at Facebook," Proc. of the 2011 International Conference on Management of Data (SIGMOD'11) Athens, Greece.
- [3] Jubatus. <http://jubat.us>
- [4] NTT press release. <http://www.ntt.co.jp/news2011/1110e/111026a.html>
- [5] R. McDonald, K. Hall, and G. Mann, "Distributed Training Strategies for the Structured Perceptron," Proc. of the 2010 Annual Conference of the North American Chapter of the ACL, pp. 456–464, Los Angeles, California, USA.
- [6] G. Mann, R. McDonald, M. Mohri, N. Silberman, and D. Walker, "Efficient Large-scale Distributed Training of Conditional Maximum Entropy Models," Neural Information Processing Systems (NIPS), 2009.
- [7] D. Okanohara, "Machine Learning Utilizing Large-scale Data by MapReduce," Hadoop Conference Japan, 2011 (in Japanese).
- [8] D. Okanohara, Y. Unno, K. Uenishi, and S Oda, "Future Prospects for Techniques Supporting Large-scale Distributed Real-time Machine Learning," WebDB Forum, Tokyo, Japan, 2011 (in Japanese).
- [9] Apache ZooKeeper. <http://zookeeper.apache.org>
- [10] T. Haerder and A. Reuter, "Principles of Transaction-oriented Database Recovery," ACM Comput. Surv., Vol. 15, No. 4, pp. 287–317, 1983.
- [11] S. Gilbert and N. Lynch, "Brewer's Conjecture and the Feasibility of Consistent, Available, Partition-tolerant Web Services," SIGACT News, Vol. 33, No. 2, pp. 51–59, 2002.
- [12] D. Pritchett, "BASE: An Acid Alternative," Queue, Vol. 6, No. 3, pp. 48–55, 2008.
- [13] K. Crammer, O. Dekel, J. Keshet, S. Shalev-Shwartz, and Y. Singer, "Online Passive-aggressive Algorithms," Journal of Machine Learning Research, 2006.



Satoshi Oda

Researcher, Cloud System SE Project, NTT Software Innovation Center.

He received the B.E. and M.E. degrees in engineering from Keio University, Kanagawa, in 2003 and 2005, respectively. Since joining NTT Information Sharing Platform Laboratories in 2005, he has been engaged in R&D of information security, fast implementation of cryptography, and security protocols. As a result of organizational changes in April 2012, he is now in NTT Software Innovation Center. He received the 2007 Outstanding Presentation Award from the Japan Society for Industrial and Applied Mathematics (JSIAM) and the 2009 Life Intelligence and Office Information System (LOIS) Research Award. He is a member of JSIAM.



Kota Uenishi

Engineer, Distributed Data Processing Platform Project, NTT Software Innovation Center.

He received the B.E. degree in engineering and the M.S. degree from the Department of Frontier Informatics at the University of Tokyo in 2005 and 2007, respectively. He joined NTT Information Sharing Platform Laboratories in 2007. Since 2008, he has been engaged in R&D of fault-tolerant distributed computing systems for a search engine backend. As a result of organizational changes in April 2012, he is now in NTT Software Innovation Center.



Shingo Kinoshita

Senior Research Engineer, Supervisor, Group Leader, Distributed Computing Project, NTT Software Innovation Center.

He received the B.E. degree in solid state physics engineering from Osaka University in 1991. Since joining NTT Information and Communication Systems Laboratories in 1991, he has been engaged in R&D of fault-tolerant distributed computing systems, Internet protocols, especially a reliable multicast protocol, information security, especially RFID privacy protection technology, and big data computing. During 2006–2007, he studied the management of technology at University College London and received the M.Sc. degree in 2007. During 2008–2011, he worked in human resources in the planning section of the laboratories. He is currently managing distributed computing projects including Hadoop, Jubatus, and the mobile cloud computing technology Virtual Smartphone. As a result of organizational changes in April 2012, he is now in NTT Software Innovation Center. He received the 2005 Information Processing Society of Japan (IPJS) Research and Development Award, the 2003 IPJS Symposium CSS Best Paper Award, the 1998 IPJS Symposium DiCoMo Best Presentation Award. He is a member of IPJS and the steering committee of IPJS SIG-DPS.

Standardization Activities Related to Machine-to-Machine Communications

Tomoki Omiya[†] and Naomi Orimo

Abstract

Machine-to-Machine (M2M) communications, which enables autonomous information exchange between machines via telecommunications networks, is currently receiving attention from diverse industries as a valid mechanism for supporting the future information society. M2M-related services are being launched by telecommunications operators in Japan and abroad, and relevant standardization activities are in progress at a number of standardization organizations and forums. This article mainly introduces M2M-related trends and M2M standardization activities.

1. Introduction

Various efforts using Machine-to-Machine (M2M) communications as a common infrastructure are being widely made towards information infrastructures for the next-generation society. Driven by EU directives and legislation in Europe and a number of economic policy initiatives set out by the Obama administration of the USA for reducing energy consumption, utilizing renewable energy sources, reducing environmental load, reducing traffic congestion, and eradicating traffic accidents, efforts to achieve an information infrastructure for the future information society through the use of smart grids and smart cities are taking place on a global scale. For instance, the introduction of the eCall system (emergency call system) and smart metering system in Europe and the USA, as well as the introduction of vehicle theft prevention measures in Brazil, have been driven by national policies.

With M2M, various *machines* that are currently not connected to networks will be connected, thereby enabling us to make use of the information collected from them for the provision of information that is useful to users. For this reason, M2M is becoming increasingly popular in various industry sectors.

For instance, the Intelligent Transportation Systems (ITS) developed by the automotive industry can con-

tribute to the reduction of CO₂ emissions by providing realtime road traffic information, which should help to shorten traveling time and distance. Furthermore, information exchanged between vehicles and infrastructure elements or among vehicles can be used to recognize and avoid high-risk situations, which will result in fewer traffic accidents. For this purpose, standardization for Driving Safety Support Systems using the 700-MHz band is currently in progress in Japan. As a part of ITS, telematics offerings utilizing in-vehicle information technologies are also becoming successful. Another good example can be seen in the area of telemedicine/telehealthcare. Telemedicine enables swift and prompt responses to emergencies as well as lower labor costs. And with the aging of the world's population, future demands for telemedicine/telehealthcare services are expected to rise still further. M2M utilization aimed at speeding up and improving efficiency is also becoming increasingly active in various industry sectors, such as the logistics industry (for tracing baggage and commercial goods), the electrical power industry (for smart metering and smart grids), the insurance industry (for tracing and locating stolen vehicles), and the security industry (for remote monitoring and control).

M2M communizes networks and platforms against the background of social and industrial demands, and it will create attractive business opportunities for telecommunications operators. Furthermore, from the perspective of ensuring mobility and facilitating

[†] NTT Advanced Technology Corporation
Musashino-shi, 180-0006 Japan

connectivity, wireless technology such as mobile communications and short-range wireless communications will play an important role in M2M.

As one activity communizing M2M, studies on international standards by major Standards Development Organizations (SDOs) such as ETSI (European Telecommunications Standards Institute) are becoming active, and M2M-related industrial trends and standardization activities are now receiving attention.

2. M2M issues for telecommunications operators

Taking into account the growing interests in various industry sectors for using M2M and new deployments of M2M equipment invoked by national legislation, the number of M2M devices is expected to increase sharply in the future. For instance, Cisco Systems, Inc. forecasts that by 2020, the number of devices connected to the Internet will reach 50 billion [1], of which the majority will be M2M-related devices. This figure indicates that, in comparison with the current number of global mobile subscriptions, which is around 5.4 billion [2], M2M devices of the next higher order of magnitude will be connected to the Internet by 2020. In addition to this, the range of network traffic needed by M2M devices varies widely from one M2M application to another: for instance, the volume of traffic generated by sensor equipment will be low, while that generated by security surveillance cameras will be relatively high. Supporting the enormous number of M2M devices to be connected and efficiently covering the wide range of traffic volume are challenging issues for telecommunication operators.

3. Background of M2M standardization

While traditional M2M systems are mainly vertically integrated systems specifically optimized for a particular industry sector or solution, horizontally integrated systems, which could be commonly used within and across any industry sector or solution, are becoming important. Therefore, M2M systems that support a variety of services are collections of technological elements that meet requirements from a very wide range of industry sectors (vertical players). The technical areas related to M2M standardization activities by major SDOs are shown in **Fig. 1**. They are broadly categorized into four domains: devices and gateways, access and core networks, platforms, and applications. Studies take a cross-category

approach based on an end-to-end perspective.

3.1 Devices and gateways

There are two arrangements for supporting M2M device connectivity: either connection directly to telecommunications operator networks or connection via gateways located in home networks or elsewhere. Since sensors and actuators used for M2M applications are required to have low power consumption and long operating lives, various short-range wireless communications technologies such as Z-Wave, ANT+, ZigBee, and Bluetooth have been studied.

3.2 Access and core networks

It is assumed that existing technologies for access networks such as mobile, wireless, and fixed-line network technologies will be reused for M2M. In addition to mobile communications technologies, automotive wireless technologies such as DSRC (Dedicated Short-Range Communications) used by ITS hotspot services are also being studied for automotive use cases. The type of technology used will vary depending on the equipment's mobility and the criticality of emergency situations. For example, in the case of the eCall system for vehicles, mobile communications technology is promising as access technology because of its high level of mobility and high level of criticality for emergencies. Another case where mobile communications technology is also widely used is automatic vending machines because it facilitates their installation in various locations even though they remain immobile for most of the time. On the other hand, consumer electronics equipment, which requires only limited mobility and is installed in a limited range of locations, will be connected via short-range wireless to a home gateway supported by optical fiber access.

Core networks, on the other hand, require mechanisms for identifying a huge number of devices and performing efficient routing, as well as technology for efficiently handling a wide range of traffic volume.

3.3 Platforms

Studies of platforms are currently in progress to examine the functions required for the provision of application services from a variety of industry sectors, as well as studies of the basic Application Programming Interfaces (APIs) commonly used regardless of the industry sector. As for the arrangement of platform provision, noteworthy studies include the horizontally integrated cloud platform approach

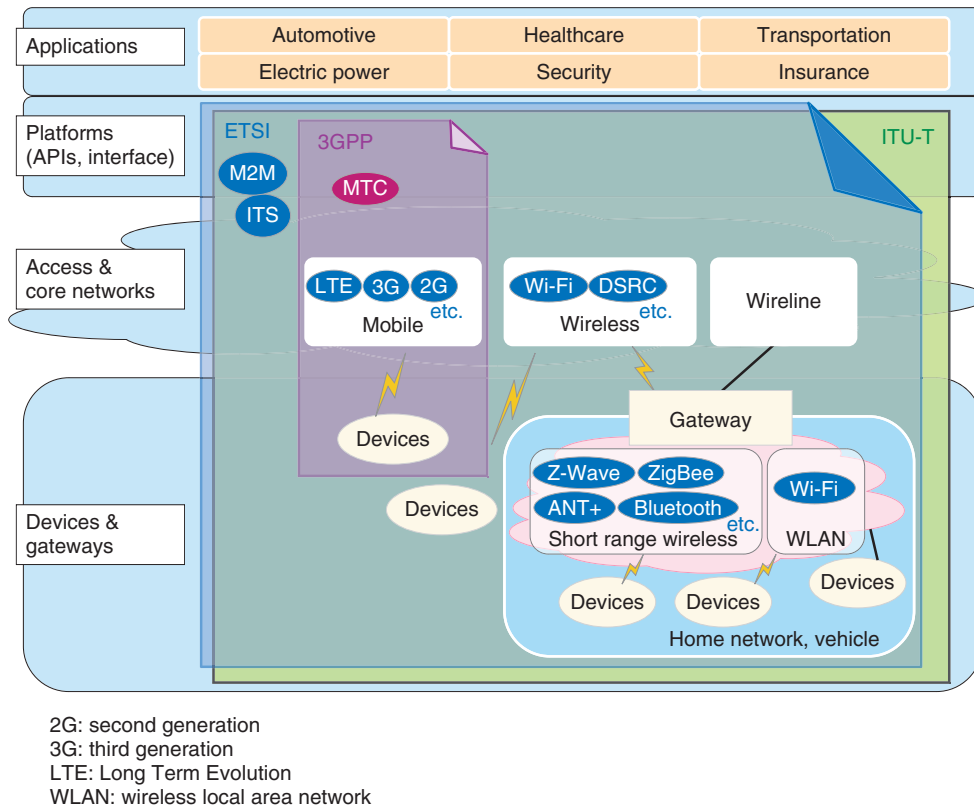


Fig. 1. M2M technical areas and major SDOs.

making use of cloud-computing technology to be commonly used within any industrial sector and across any industry sectors.

3.4 Applications

Similar use cases are currently being examined by among various SDOs. Applications considered suitable for each industry sector are shown in Fig. 1.

4. Current status of major M2M standardization activities

Standardization activities covering M2M-related technical issues are currently under development by various SDOs and forums. This section provides a brief summary of the activities undertaken by the major organizations shown in Fig. 1. A study of this area under the title “Internet of Things” (IoT) has been started by ITU-T (International Telecommunication Union, Telecommunication Standardization Sector). The term IoT is also used in the EU Framework Programme 7 project.

4.1 3GPP

3GPP (3rd Generation Partnership Project) started standardization activities on mobile network-based M2M in September 2008 under the title “Machine Type Communications” (MTC). This study is regarded as one of the most advanced studies of M2M.

3GPP Release 10 specifications approved in March 2011 cover use cases, service requirements, and a functional architecture for MTC intended for application to mobile networks. In this release, 3GPP standardized overload and congestion controls for networks and secure telecommunication functions for MTC devices in roaming environments in order to cope with new traffic characteristics caused by collecting small amounts of information at the same time from a huge number of MTC devices, which has not previously been done in existing human-oriented telecommunication. Technical documents covering the service requirements and architectural model have also been issued as TS 22.368 and TR 23.888, respectively.

At present, issues such as group-based MTC device

management capabilities and communications between MTC devices are being studied under a new work item entitled System Improvements to Machine-Type Communications (SIMTC).

4.2 ETSI

4.2.1 TC M2M

In accordance with EU Mandates M/441 (on smart metering) and M/490 (on smart grids) issued by the European Commission, ETSI established ETSI TC M2M (Technical Committee M2M) in January 2009 to develop European standards covering M2M. TC M2M is currently studying use cases, service requirements, architecture, and interfaces at the M2M service layers considering the independence of end-to-end services from access technology. Study work on M2M use cases covers five M2M application areas: smart metering, eHealth, connected consumers, automotive, and city automation. One Technical Report (use cases for smart metering) has already been published as TR 102 691.

TC M2M initiated work on detailed technical issues in 2011, and Release 1 specifications were approved by February 2012. Technical Specifications covering M2M service requirements, architecture, and interfaces have already been published as TS 102 689, TS 102 690, and TS 102.921, respectively.

4.2.2 TC ITS

In October 2007, ETSI established TC ITS (Technical Committee ITS) to standardize ITS/telematics covering the study outputs from the EU Framework Programme project. While the dominant members of TC M2M are telecommunications operators, dominant members of TC ITS are vehicle manufacturers.

In June 2009, TC ITS published TR 102 638, which defines the Basic Set of Applications (BSA) for ITS across Europe. This was followed in September 2010 by the publication of TS 102 637-1, which specifies the functional requirements driven by applications and their use cases defined in the BSA. These technical specifications identify a total of 32 use cases categorized into 7 applications in 4 application classes.

4.3 IETF

In IETF (Internet Engineering Task Force), an informal Bar BOF (birds of a feather) on IoT research issues was held at IETF 77 March 2010. Research is merely at the preliminary stage of calling for the need to study IoT, on the basis of individual drafts, and trying to identify issues that may arise in the case of connecting various things, such as radio-frequency identification tags to the Internet.

4.4 ITU-T

ITU-T's Telecommunication Standardization Advisory Group (TSAG) agreed to establish a Global Standards Initiative on the Internet of Things (IoT-GSI) at the February 2011 meeting. IoT-GSI comprises relevant Questions from Study Groups, and at its first meeting held in May 2011, IoT-GSI began a study mainly targeting IoT definitions, IoT overviews, and an IoT work plan for deploying IoT. The third IoT-GSI meeting held in November 2011 almost completed the draft ITU-T Recommendation "IoT Overview", which covers the definition of terms including IoT definition, general overview, requirements, and the architecture. Activities of the EU Framework Programme 7 project are also recognized, and coordination has started. Three draft ITU-T Recommendations—Overview of Internet of Things, Requirements for support of machine oriented communication applications in the NGN environment, and Framework of object-to-object communication for ubiquitous networking in NGN—began the approval procedure as Y.2060, Y.2061, and Y.2062, respectively, at the SG13 meeting held in February 2012 (NGN: Next Generation Network).

5. Coordination among standardization activities

Up to now, standardization efforts including those for M2M applications have been undertaken separately by regional standardization organizations in Europe, the USA, Asia, etc. These activities are leading to fears of a tightness of work resources from industries and of market fragmentation. From this standpoint, a movement to internationally integrate M2M-application-related standardization activities has been seen.

5.1 M2M consolidation

ETSI agreed to the establishment of M2M-PP (M2M Partnership Project) at the General Assembly held in April 2011 in order to avoid overlapping efforts for common M2M service-layer standardization activities among various SDOs; this was later followed by the setting up of the Board M2M-PP in ETSI. Like 3GPP, M2M-PP is intended to be a *partnership project* of several SDOs. In response to an appeal by ETSI, SDOs from different countries held preparatory meeting officially three times in 2011 (July 2011 in Seoul, Korea; August 2011 in Washington D.C., USA; and December 2011 in Berlin, Germany) targeting the establishment of M2M consolidation. SDOs are currently exchanging views

towards the consolidation of various M2M standardization activities, including the scope of activity and organization structure. Participating SDOs are: ETSI from the EU, ATIS (Alliance for Telecommunications Industry Solutions) and TIA (Telecommunications Industry Association) from the USA, CCSA (China Communications Standards Association) from China, TTA (Telecommunications Technology Association) from Korea, and TTC (The Telecommunication Technology Committee) and ARIB (Association of Radio Industries and Businesses) from Japan.

ETSI initially planned the first meeting of the new consolidated organization to be launched by early December 2011; however, the establishment of this new organization has been delayed owing to a counter proposal for an M2M Global Initiative from SDOs in the USA concerned about avoiding EU-centric management. Finally, in January 2012, the above-mentioned seven SDOs officially announced agreement to establish a new organization called oneM2M [3]. The fourth preparatory meeting was held in Tokyo in March 2012, where agreements including management and funding arrangements were planned for July and an initial technical meeting was planned for September.

Since it is recognized that engaging and partnering the vertical market players is important, a key factor for success will be how many vertical market players from various industry sectors become involved in the oneM2M activities. This deserves close attention.

6. Major issues related to future M2M standardization

There is a growing need to establish a flexible way to identify the vast number of M2M devices and routing methods for them. Another major issue to be

addressed is ensuring security by the networks to prevent devices from being stolen and information leaking through attacks on networks.

The volume of traffic exchanged during a single M2M communication session is considered, in general, to be small; therefore, if session-based communications like SIP (session initiation protocol) were to be used each time, it would result in a large overhead that could lead to network congestion. Therefore, simplified methods of communication control and congestion control are also considered to be issues that need to be solved.

Another important issue is how to design APIs for services from various industry sectors and how to profile various standard technologies.

7. Conclusion

M2M standardization has just started towards services from various industry sectors integrated horizontally. From a practical viewpoint, however, the creation of a common place for discussion involving various industry sectors that have traditionally had different backgrounds will be a key factor not only for the success of this effort, but also for the provision of commonly used functionalities and for cooperation with applications by telecommunications operators beyond the provision of basic connectivity. This article is based on information obtained through the support business for the NTT R&D laboratories.

References

- [1] <http://blogs.cisco.com/news/the-internet-of-things-infographic/>
- [2] Ed. by InfoCom Research, Inc., "Information & Communications in Japan 2012," p. 184, NTT Publishing Co., Ltd., 2011.
- [3] oneM2M (site still under construction as of June 2012). <http://onem2m.org/>



Tomoki Omiya

Senior Manager, Network Technology Center, NTT Advanced Technology Corporation.

Since joining Nippon Telegraph and Telephone Public Corporation (now NTT) in 1979, he has been active in network architectures, protocols, and interconnection interfaces for various networks including ISDN and NGN. He has also been an active executive in standardization such as ITU-T and TTC. He received awards from the Telecommunication Advancement Foundation (Japan) and the ITU Association of Japan in 1987 and 2005, respectively. He moved to NTT Advanced Technology Corporation in 2005.



Naomi Orimo

Deputy Senior Engineer, Network Technology Center, NTT Advanced Technology Corporation.

Since joining NTT Advanced Technology Corporation in 2002, she has been working on the development of voice quality measurement tools for VoIP, and since 2007, she has also been engaged in SIPv6 promotion activities at the Certification WG of the IPv6 Promotion Council in Japan. She is currently working on M2M standardization trends and technology research.

Cable Damage during Deicing of a Handhole

Abstract

This article introduces a case study of cable damage during the deicing of a handhole and offers recommendations for damage-free deicing. It is the eleventh in a bimonthly series on the theme of practical field information about telecommunication technologies. This month's contribution is from the Materials Engineering Group, Technical Assistance and Support Center, Maintenance and Service Operations Department, Network Business Headquarters.

1. Introduction

NTT telecommunication facilities are deployed far and wide throughout Japan. They include many man-holes, handholes, and similar facilities where water can easily accumulate, and in cold regions, may freeze during the winter months. This article introduces a case study of deformation and damage to the outer sheath of an optical cable that occurred during deicing of the interior portion of a frozen handhole in a cold region of the country to enable maintenance work to be performed.

2. Circumstances and inspection

2.1 Background

In February 2011, a company associated with the electrical power system was deicing an NTT handhole located in a mountainous area. During this work, the plastic portion of the sheath covering an NTT optical cable (40SM-WBB) was deformed into fibrous threads and the cable itself was damaged not only on its surface but also in its inner portion to the extent of an open cut (**Figs. 1 and 2**). This deicing was carried out using typical deicing tools (such as scrapers and sharp-edged tools) and a high-pressure water sprayer (water temperature: 30°C; nozzle pressure: 18 MPa).



Fig. 1. Handhole prior to deicing.



Fig. 2. Damaged optical cable with open cut.

† NTT EAST
Ota-ku, 144-0053 Japan

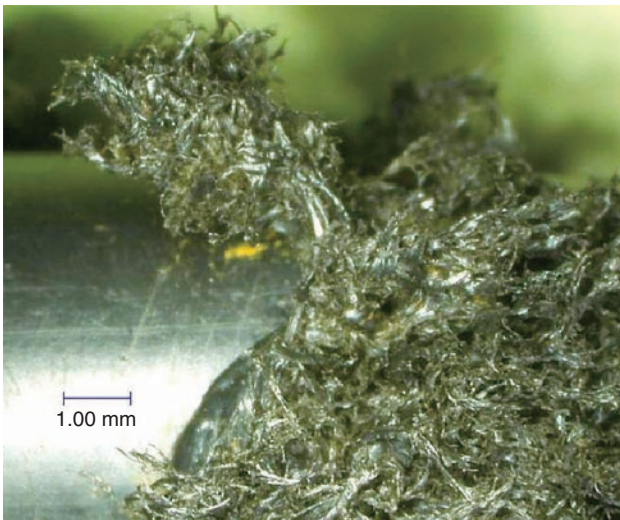


Fig. 3. Magnified view of cut in damaged optical cable.



Fig. 4. Cable damaged by a sharp-edged object.



Fig. 5. Damage-reproduction experiment using a high-pressure water sprayer.

2.2 Inspection

As shown in Fig. 2, the outer sheath of the cable was severely damaged at a particular section that turned fibrous. A magnified view of the damaged section taken with a microscope is shown in Fig. 3. Apart from this section, the cable did not incur any damage, and since the boundaries of the damaged section were clearly discernible, it was surmised that the damage was caused by localized application of external physical force.

3. Damage-cause investigation and damage-reproduction experiment

3.1 Destructive test using a sharp-edged tool

Since the mechanical outer damage might have been caused by deicing tools, we guessed that the deicing in this case was performed using either a sharp-edged tool conveniently at hand or a special-purpose deicing scraper onsite. However, when we scraped at the outer sheath of the cable using a saw-like tool, we found that only simple cuts were formed without any fibrous threads (Fig. 4).

3.2 Destructive test using a high-pressure water sprayer

NTT-related business operators perform the same kind of deicing operation by spraying unpressurized warm water at a temperature of about 60°C. However, because a high-pressure water sprayer was used at the time of the accident, we decided to use a machine of the same type in an experiment designed to try and reproduce the damage. Specifically, we used a high-pressure water sprayer (Seiwa Sangyo jet-boiler/jet-clean product) to spray a new 40SM-WBB cable on the premises of the Technical Assistance and Support Center (Fig. 5). In this experiment, we varied two parameters: the nozzle pressure and the distance between the nozzle and cable. The results are given in Table 1.

Initially, we set the water temperature to about 30°C and nozzle pressure to 18 MPa and reproduced the working conditions at the site of the accident. We found that spraying the cable with water for 15 s from a distance of 5 cm damaged the outer sheath of the cable turning it fibrous, as shown in Fig. 6. From this result, we concluded that deicing performed using a high-pressure water sprayer was the cause of the damage in this incident.

We then performed additional testing to determine what usage conditions and usage method would avoid causing such damage. We found that when the nozzle-

Table 1. Experimental conditions and damage to cable surface.

Nozzle pressure	18 MPa	9 MPa	4.5 MPa
Temperature	30°C	30°C	30°C
Nozzle-to-cable distance: 1 cm	Severe damage	–	No damage
Distance: 5 cm	Severe damage	Severe damage	No damage
Distance: 15 cm	Minute cracks	No damage	–
Distance: 30 cm	No damage	No damage	–

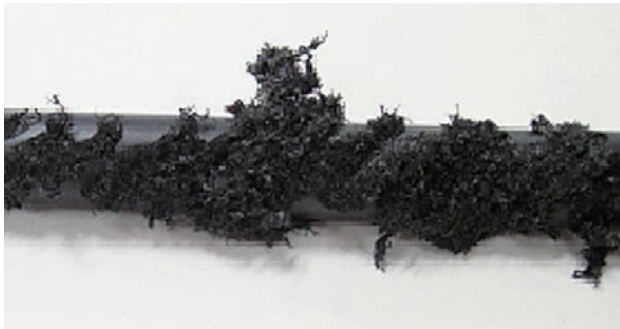


Fig. 6. Cable with damage reproduced (18 MPa, 30°C, 5 cm).

to-cable distance was 15 cm, minute cracks appeared; however, when the distance was 30 cm, no damage occurred. This led us to conclude that damage can be prevented in future if the distance from the nozzle to the ice (cable) is 30 cm or greater.

We did not observe any major changes in the damage produced when the nozzle pressure was reduced to 9 MPa, but we found that no damage occurred when it was reduced to 4.5 MPa, even when the ice was sprayed at close range. Thus, while this experi-

ment does not constitute detailed testing, the results indicate that no cable damage will occur at pressures at or below a certain value.

4. Summary of findings

From our experimental results, we conclude that using a high-pressure water sprayer to deice a hand-hole can damage a cable and turn its outer sheath fibrous. We also found that such damage can be avoided by reducing the pressure of the high-pressure water sprayer to 4.5 MPa or setting the distance from the nozzle to the cable to 30 cm or greater. However, as actual conditions may differ depending on equipment specifications such as the shape of the nozzle tip, it is not possible to firmly establish safe parameters for using a high-pressure water sprayer. We therefore recommend that the use of a high-pressure water sprayer be avoided if at all possible.

In short, we strongly recommend that the deicing of telecommunications facilities containing NTT cables should be done by spraying with unpressurized warm water (about 60°C). This method conforms to the standard NTT deicing procedure.

5. Conclusion

This article presented a case study of cable damage in a cold region in Japan. We hope that the information provided here has enhanced our reader’s understanding of material deterioration. Various telecommunications facilities suffer deterioration or damage in addition to the handholes described here. Please feel free to consult with NTT EAST Technical Assistance and Support Center in the event of a facility fault or deterioration-related problem with an unknown cause.

External Awards

JSAP Outstanding Presentation Award

Winner: Nobuyuki Matsuda, NTT Basic Research Laboratories

Date: May 11, 2012

Organization: The Japan Society of Applied Physics (JSAP)

For “Integrated Polarization-entanglement Source on a Chip”.

Quantum entanglement is a quintessential resource for quantum information systems, such as ones for quantum communication and quantum computation. A recent integrated-photonics approach for large-scale photonic quantum information processing provides a stable path length and a compact physical size. Since a number of quantum information protocols are based on the polarization degree of freedom, it is crucial to develop building blocks for generating, manipulating, and analyzing the polarization-entangled states of photons on a chip. Here, we report an integrated waveguide source that *generates* photon polarization entanglement for the first time. By using silicon photonics technology developed for on-chip optical interconnections, we monolithically implemented the polarization-entanglement source on a silicon chip.

Poster Awards for Both Excellent Poster Presentation and Poster Preview Presentation at International Conference on Topological Quantum Phenomena

Winner: Hiroshi Irie, NTT Basic Research Laboratories

Date: May 20, 2012

Organization: Organization Committee of TQP2012

For “Josephson Characteristics of Superconducting Quantum Point Contact”.

A superconducting quantum point contact (SQPC) is a Josephson junction consisting of a semiconductor quantum point contact (semiconductor QPC) embedded in a narrow gap between two superconducting electrodes. It has been theoretically demonstrated that the critical current in an SQPC shows a steplike variation, reminiscent of the conductance quantization in a semiconductor QPC. Early experimental effort partly demonstrated such discretization of the critical current, although the visibility of the stepwise change was low and the study was limited to the multichannel regime because of the inferior gating properties of QPCs. In this study, we improved gate controllability, which resulted in an unambiguous demonstration of the discretization for the first time.